AGU
ADVANCING EARTH AND SPACE SCIENCE

JGR Biogeosciences

Key Points:
- Across a latitudinal gradient, landscape characteristics exert major controls on dissolved organic matter composition in northern watersheds
- Watersheds underlain by continuous permafrost export less dissolved organic carbon that is less aromatic
- Across latitudes a deeper seasonally thawed active layer may contribute higher proportions of terrestrial organic matter to northern rivers

Supporting Information:
Supporting Information may be found in the online version of this article.

Correspondence to:
S. E. Johnston,
sarahellenjohnston@gmail.com

Author Contributions:
Conceptualization: Sarah Ellen Johnston, Joanna C. Carey, Robert G. M. Spencer
Data curation: Sarah Ellen Johnston, Robert G. M. Spencer
Funding acquisition: Joanna C. Carey, Robert G. M. Spencer
Investigation: Sarah Ellen Johnston, Joanna C. Carey
Methodology: Sarah Ellen Johnston, David C. Podgorski
Project Administration: Robert G. M. Spencer
Supervision: Joanna C. Carey, Robert G. M. Spencer
Visualization: Sarah Ellen Johnston, Anne Kellerman, Jonathan Gewirtzman
Writing – original draft: Sarah Ellen Johnston, Robert G. M. Spencer

Controls on Riverine Dissolved Organic Matter Composition Across an Arctic-Boreal Latitudinal Gradient

Sarah Ellen Johnston[1,2], Joanna C. Carey[3], Anne Kellerman[1], David C. Podgorski[1,4], Jonathan Gewirtzman[5,6], and Robert G. M. Spencer[1]

[1]National High Magnetic Field Laboratory Geochemistry Group and Department of Earth, Ocean, and Atmospheric Science, Florida State University, Tallahassee, FL, USA, [2]Now at: Department of Biological Sciences, University of Lethbridge, Lethbridge, AB, Canada, [3]Division of Math & Science, Babson College and Department of Earth and Environment, Boston University, Boston, MA, USA, [4]Now at: Department of Chemistry, Pontchartrain Institute for Environmental Sciences, Shea Penland Coastal Education & Research Facility, Chemical Analysis & Mass Spectrometry Facility, University of New Orleans, New Orleans, LA, USA, [5]Department of Biology, Boston University, Boston, MA, USA, [6]Now at: Yale School of the Environment, Yale University, New Haven, CT, USA

Abstract Climatic changes are transforming northern high-latitude watersheds as permafrost thaws and vegetation and hydrology shift. These changes have implications for the source and reactivity of riverine dissolved organic matter (DOM), and thus biogeochemical cycling, across northern high-latitude systems. In this study, we use a latitudinal gradient from the interior to the North Slope of Alaska to evaluate seasonal and landscape drivers of DOM composition in this changing Arctic environment. To assess DOM source and composition, we used absorbance and fluorescence spectroscopy to measure DOM optical properties, lignin biomarker analyses to evaluate vascular plant contribution to the DOM pool, and Fourier transform ion cyclotron resonance mass spectrometry (FT-ICR MS) to assess DOM compositional changes. We found that seasonal inputs of DOM at elevated discharge during the freshet were typically more aromatic in nature with higher lignin concentrations and carbon-normalized yields. Landscape characteristics were a major control on dissolved organic carbon (DOC) yields and DOM composition. More northern watersheds, which were steeper, underlain by continuous permafrost, and exhibited a mix of barren and lichen/moss vegetation cover, exported less DOC with relatively more aliphatic DOM compared to more southern basins. Watersheds with deeper active layers exported DOM that was more aromatic with higher polyphenolic and condensed aromatic relative abundances and lignin yields, likely sourced from shallow subsurface flow during high discharge periods. However, contributions from deeper groundwater to streamflow is expected to increase, which would increase interactions of groundwater with mineral soils and decrease aromatic DOM contributions during periods of low discharge.

Plain Language Summary Northern high-latitude rivers are undergoing changes linked to thawing permafrost, warming temperatures, and altered hydrology due to climate change. These changes will impact the source and cycling of carbon in these rivers. Here, we analyzed dissolved organic matter (DOM) composition from watersheds across a gradient of permafrost and vegetation coverage to assess how northern high-latitude rivers will respond to change. This gradient of time and space enabled us to project how watersheds might respond to climatic changes. We hypothesized that sites with continuous permafrost north of the tree line export less dissolved organic carbon and DOM that is less terrestrial, due to longer subsurface residence that enhances processing of terrestrial DOM. Consistent with this hypothesis, the sparsely vegetated, steep northern watersheds underlain by continuous permafrost contained DOM characteristic of snowmelt or groundwater. Conversely, more forested, southern basins contained more terrestrial DOM. As these watersheds change the contribution of shallow subsurface flow might increase DOC exports and the contribution of terrestrial DOM, with the caveat that deeper groundwater contributions with altered hydrology can decrease DOC and terrestrial inputs in these systems.

Writing – review & editing: Joanna C. Carey, Anne Kellerman, David C. Podgorski, Jonathan Gewirtzman, Robert G. M. Spencer

1. Introduction

Northern high-latitude regions are experiencing rapid changes due to climate change that are impacting carbon (C) cycling and biogeochemical processing in these regions (McGuire et al., 2009). The northern high-latitude landscape contains abundant surface water, including lakes and rivers, vulnerable to climatic changes (Bring et al., 2016; Verpoorter et al., 2014). Arctic rivers transport approximately 34 Tg C to the Arctic Ocean annually, representing a major flux of dissolved organic carbon (DOC) to the global oceans (Holmes et al., 2012; Johnston et al., 2018; Mann et al., 2016). Rivers act as important sites of biogeochemical processing and integrate the biogeochemical signals from terrestrial and aquatic ecosystems across the landscape (Battin et al., 2009; Cole et al., 2007; Drake et al., 2018). Changes associated with climatic warming, including permafrost thaw, ecological succession, and a longer growing season, are projected to alter the transport and reactivity of C in these rivers (Abbott et al., 2016; Hu et al., 2010; Jorgenson et al., 2013; O'Donnell et al., 2012; Vonk, Tank, Bowden, et al., 2015). Thus, understanding the sensitivity of northern high-latitude rivers to these changes across a gradient of latitudes and landscape characteristics is critical to predict the future C balance of the Arctic under climatic warming.

Northern high-latitude river hydrology is driven by seasonal snowmelt in the spring, delivering a large proportion of the annual flux of DOC and terrestrial dissolved organic matter (DOM) during the freshet, the period of high discharge during snow and ice melt (Holmes et al., 2012; Kaiser et al., 2017; Stedmon et al., 2011). Over 50% of the annual water yield in large Arctic rivers occurs during the freshet, coinciding with the period of maximum DOC export (Amon et al., 2012; Holmes et al., 2012). Later in the summer months, the active layer thaws and permafrost may thaw, shifting hydrologic flowpaths deeper in the soil profile and causing greater interaction between shallow and deep groundwater and surface waters (Bring et al., 2016; Koch et al., 2013; Walvoord et al., 2012). As the active layer thaws seasonally, subsurface flow paths shift from organic to mineral soil horizons, this shift is associated with a higher relative contribution of less aromatic DOM from groundwater sources compared to other DOM sources (Bring et al., 2016; McClelland et al., 2007; O'Donnell et al., 2012; Walvoord & Striegl, 2007). Regions underlain by discontinuous permafrost are particularly vulnerable to rising soil temperatures, as soil temperatures are closer to thawing temperatures and changes in discontinuous permafrost extent have been recently observed (Jorgenson et al., 2001). The diminished extent of discontinuous permafrost and shifts from continuous to discontinuous permafrost regions will have implications for hydrology and DOM composition (Frey & McClelland,, 2009; Loranty et al., 2018; O'Donnell et al., 2012; Schuur et al., 2013). Groundwater plays an important role in contributing DOM to northern high-latitude rivers (Connolly et al., 2020). For example, approximately one quarter of the annual discharge to the Yukon River is from groundwater, with higher contributions from groundwater during the under-ice period (Walvoord & Striegl, 2007). Increasing groundwater contribution to streams across Alaska has been implicated in decreasing DOC concentrations and increasingly biolabile DOM in streams and rivers (O'Donnell et al., 2012; Striegl et al., 2005; Walvoord & Striegl, 2007).

In addition to changes in DOM composition associated with shifts in groundwater contributions, thawing permafrost can alter the quality of DOM released from the terrestrial landscape (O'Donnell et al., 2014, 2016). Laboratory incubations demonstrate that permafrost can release highly biolabile DOM, with up to 50% loss of DOC over a 28-day period (Mann et al., 2012; Spencer et al., 2015; Vonk, Tank, Mann, et al., 2015). Permafrost thaw is also likely to increase the export of low molecular weight, biolabile DOC to rivers (Drake et al., 2015; Spencer et al., 2015) containing aged vascular plant derived DOM (Feng et al., 2017). Landscape scale changes, including the lengthening of the ice-free season, the northward progression of vegetation, and wildfires will also impact the composition, concentration, and sources of DOM transported in Arctic rivers (Abbott et al., 2016; Rodriguez-Cardona et al., 2020; Stubbins et al., 2015), however the response to these changes is uncertain across the complex landscape (Loranty et al., 2018).

In fluvial ecosystems, DOM composition varies throughout the river network from headwaters to large rivers and with latitude (Casas-Ruiz et al., 2020; Kawahigashi et al., 2004; Massicotte et al., 2017), however many studies of northern high-latitude rivers have focused on large river systems. The composition and reactivity of DOM is tightly linked to its source and processing (D'Andrilli et al., 2015; Kellerman et al., 2018). Changes in the source and thus composition of DOM have implications for the biogeochemical role and fate of DOM, impacting C cycling in these northern watersheds. Recent advances in mass spectrometry allow

the identification of DOM composition at ultrahigh resolution via Fourier transform ion cyclotron resonance mass spectrometry (FT-ICR MS). Together with the measurement of quantitative biomarker techniques, such as lignin phenols, which are unique tracers of vascular plant inputs, these analyses give us new insights into DOM composition and sources across the landscape (Amon et al., 2012; Kellerman et al., 2018; O'Donnell et al., 2016). Past studies have also found strong relationships of chromophoric DOM (CDOM) measurements with FT-ICR MS and lignin parameters demonstrating the utility of CDOM to rapidly assess DOM composition (Johnston et al., 2018; Kellerman et al., 2018; Spencer et al., 2008). Such optical measurements require small sample volumes, are relatively inexpensive, and can be done *in situ* at high temporal resolution or via remote sensing techniques to improve spatial coverage (Griffin et al., 2018). Thus, such techniques offer great potential for improving our understanding of changing DOM composition across broad temporal and spatial scales.

To examine the seasonal and environmental drivers of DOC concentration and DOM composition in the boreal-Arctic transition in interior Alaska, we collected samples from six rivers across a latitudinal gradient of permafrost, vegetation cover, and mean annual temperature. Using this gradient of latitude as a substitution for time (Lester et al., 2014), our overarching goal was to assess how riverine DOM sources and fluxes might change as permafrost thaws and vegetation changes in these northern watersheds. We evaluated the composition of DOM across this latitudinal gradient using CDOM, FT-ICR MS, and lignin biomarkers. The objectives of this study were to assess: (a) the impact of seasonality on DOM composition across the boreal-Arctic latitudinal transition; (b) the landscape scale controls on DOM composition and export; and (c) the fluxes and yields of DOC and terrestrial DOM, assessed via DOC concentration, lignin and CDOM absorbance, across a latitudinal and landscape gradient. Our space-for-time experimental design across a gradient of latitude, landscape characteristics, and discharge allowed us to examine how the composition and timing of fluvial C exports will respond to projected changes in northern high-latitudes.

2. Methods

2.1. Study Site and Sample Collection

We sampled six rivers and streams within the Yukon River Basin and the North Slope of Alaska spanning a gradient of latitude from the Salcha River, just south of Fairbanks to the Sagavanirktok River on the North Slope of Alaska (Figure 1; Table 1) during the ice-free season in 2016 (May–October) and the period of peak discharge in May 2017. Methods used to derive landscape characteristics such as permafrost coverage, active layer thickness, and land cover are described in Carey et al. (2020). The watersheds are underlain by a south to north gradient of discontinuous to continuous permafrost (50%–90%, and greater than 90% underlain by permafrost, respectively). Maximum active layer thickness (ALT) ranged from 1.536 m in the Tolovana River watershed (discontinuous permafrost) to 0.108 m in the Atigun River watershed (continuous permafrost) (Table 1) (Carey et al., 2020). Sites spanned a gradient of boreal forest and tundra land cover, from forest, grass, and shrubland dominated watersheds in the south, to barren, lichen, or moss dominated watersheds in the north (Table S1). The southern, boreal forest sites (Salcha, Chena, Tolovana, and Slate) are part of the Yukon River Basin and the northern tundra sites (Atigun and Sagavanirktok Rivers) drained streams flowing out of the Brooks Range. Field sites were located at U.S. Geological Survey continuous discharge (streamflow, Q) gages so that total exports of material could be calculated. Water yield was calculated as discharge normalized to watershed area (Table S2).

At each site, samples were collected from the middle of the river into acid washed (1 M HCl) HDPE sample bottles approximately every three to four days through the freshet period from May 2, 2016 to May 29, 2016. Additional samples were collected approximately monthly throughout the ice-free season in 2016 and in May 2017 for a total of 12–14 samples per site in the southern sites and 11 samples from the Atigun and Sagavanirktok Rivers (Table 1). Samples for lignin analyses were collected every second visit due to sample volume constraints. Following collection, samples were kept cold (4°C) and in the dark until filtering (<4 h). Samples were filtered to 0.45 μm through a rinsed Geotech dispos-a-filter Versapor capsule filter into acid washed (1 M HCl) polycarbonate or HDPE bottles. Samples were stored frozen (−20°C) until analysis.
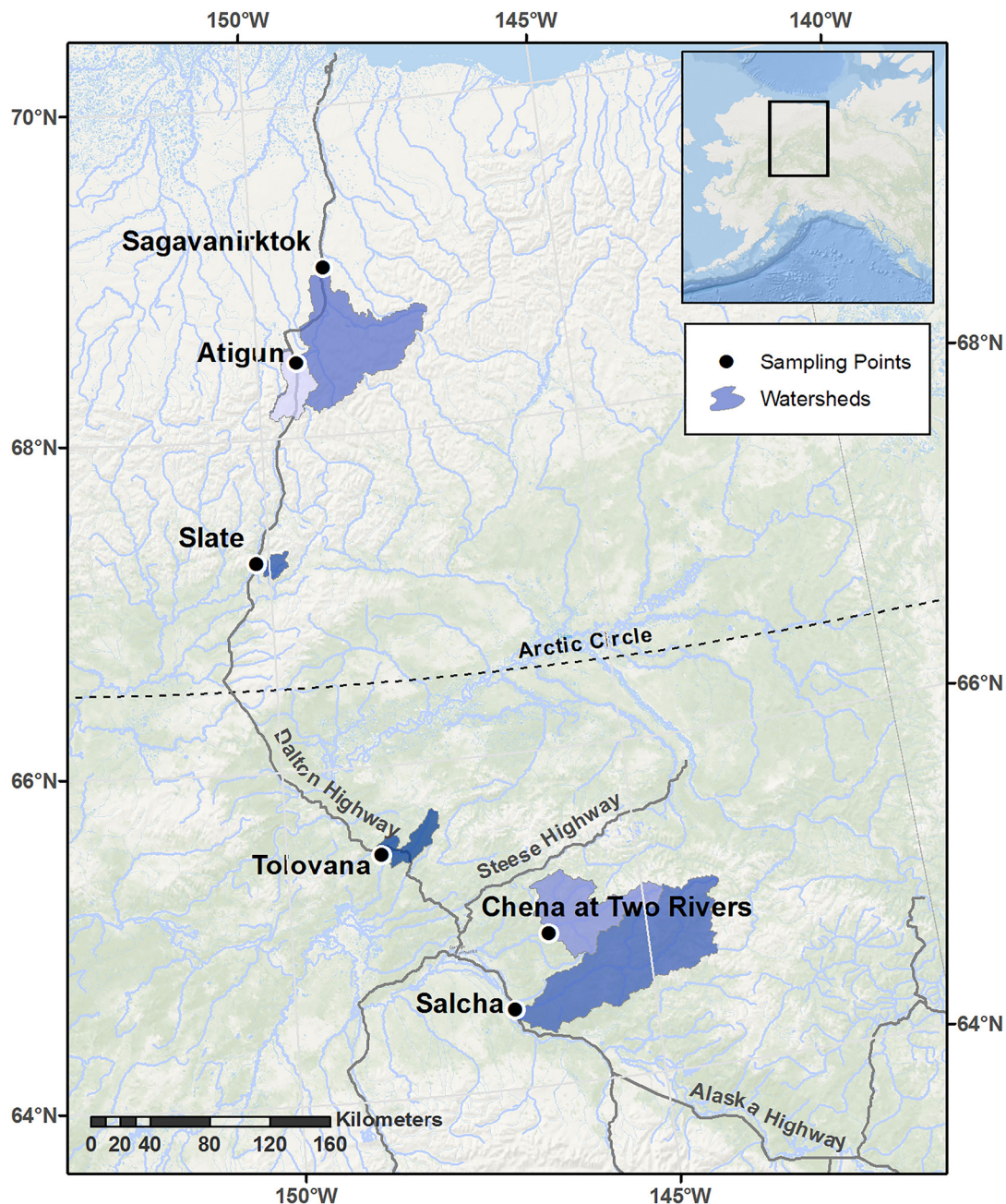
Figure 1. Map of sampling locations and watersheds.

2.2. Dissolved Organic Carbon Concentration and Optical Analyses

Filtered (0.45 μm) samples were acidified to pH 2 with 12 M HCl and analyzed for DOC concentration via high temperature catalytic oxidation on a Shimadzu TOC-L CHP. Samples were sparged for five minutes with CO_2-free air to remove dissolved inorganic carbon prior to analysis. Concentrations were calculated based on a five-point standard curve and the average of three out of seven replicate injections with a standard deviation less than 0.1 mg L^{-1} and coefficient of variation less than 1.0% using established protocols (Johnston et al., 2018).

Absorbance and fluorescence of DOM was measured on thawed, filtered water samples (0.45 μm) in a 10 mm quartz cuvette on a Horiba Aqualog at room temperature (20°C). Absorbance was measured between

Table 1
Location, Landscape Characteristics and Fluxes and Yields of DOC for Each Sample Site

USGS ID	River name	Latitude	Longitude	Drainage area (km^2)	Relief (slope, in degrees)	Mean annual discharge ($m^3\ d^{-1}\ km^{-2}$)	Permafrost zone	Average annual active layer Depth (m)	Mean annual air temperature (°C)	DOC flux (Gg y^{-1})	DOC yield (g $m^{-2}\ y^{-1}$)
	Yukon Basin										
15484000	Salcha	64°28'22"	146°55'26"	5,620	20.7	911.7	Discontinuous	1.5	0.42	18.2	3.2
15493000	Chena at Two Rivers	64°54'10"	146°21'25"	2,427	20.6	906	Discontinuous	1.0	0.02	12.6	5.1
15518900	Tolovana	65°28'19"	148°15'59"	360	10.4	578.3	Discontinuous	1.5	0.84	6.0	9.4
15564879	Slate	67°15'17"	150°10'24"	190	17.5	1,084	Continuous	1.2	−1.79	0.4	2.1
	North-Slope Basin										
15905100	Atigun	68°27'10"	149°22'06"	769	29.8	938.9	Continuous	0.1	−5.5	1.1	1.4
15908000	Sagavanirktok	69°50'23"	148°48'25"	4,817	25.5	934.4	Continuous	0.9	−5.34	8.7	1.8

wavelengths 230 and 800 nm and fluorescence was measured at excitation wavelengths from 230 to 500 nm and emission wavelengths from 230 to 800 nm. Spectra were normalized and blank corrected upon acquisition using the Aqualog software. Spectral indices were calculated using the DrEEM MATLAB toolbox (Murphy et al., 2013). Absorbance parameters included the Napierian absorption coefficient at 254 and 350 nm (a_{254} and a_{350}, respectively), indicative of CDOM in the sample, spectral slope from 275 to 295 nm ($S_{275-295}$) and from 350 to 400 nm ($S_{350-400}$), and the spectral slope ratio (S_R; $S_{275-295}$: $S_{350-400}$) related to DOM aromaticity and molecular weight (Helms et al., 2008). Fluorescence index (FI) was calculated as the ratio of the emission intensity of 470–520 nm at 370 nm excitation (Cory & McKnight,, 2005; McKnight et al., 2001), and is linked to DOM source and aromaticity. The specific UV absorbance at 254 ($SUVA_{254}$) was calculated as the DOC normalized decadic absorption coefficient at 254 nm, and is related to the aromaticity of DOM (Weishaar et al., 2003).

2.3. Solid Phase Extractions

DOM was isolated via solid phase extraction prior to FT-ICR MS and lignin phenol analyses onto separate PPL cartridges (Agilent Technologies). Filtered (0.45 μm) samples were acidified to pH 2 with 12 M HCl and PPL cartridges were soaked in methanol (>4 h) prior to extraction. For FT-ICR MS, an aliquot of filtered, acidified sample water equivalent to 40 μg OC was extracted onto 100 mg PPL cartridges (Agilent Technologies, 3 mL) and eluted with methanol for a final concentration of 50 μg OC mL^{-1} (Dittmar et al., 2008). A separate aliquot of filtered, acidified sample water was extracted for lignin, volumes were adjusted in order to extract 2.5 mg DOC onto 1 g PPL cartridges (Agilent Technologies), up to a maximum of 500 mL. Samples for lignin analyses where then eluted with 4 mL of methanol.

2.4. Lignin Phenol Biomarker Analysis

Biomarker lignin phenols were measured on a subset of samples with four to five samples analyzed for each site. Dried solid phase extracts were oxidized using cupric oxide followed by liquid-liquid extraction prior to analysis using GC-MS following established protocols (Johnston et al., 2018; Spencer et al., 2010). Briefly, dried extracts were dissolved in O$_2$-free 2M NaOH; oxidized with 500 mg cupric oxide, 75 mg ferrous ammonium sulfate, and 50 mg glucose; and heated to 155°C for 3 h. Then *trans*-cinnamic acid was added as an internal standard and samples were acidified to pH 1 with 85% H$_3$PO$_4$. Acidified oxidation products were extracted via liquid-liquid extraction into ethyl acetate, dried, and reconstituted in pyridine. Samples were then derivatized with N/O bis-trimethylsilyltrifluoromethylacetamide and 1% trimethylchlorosilane at 60°C for 10 min and analyzed on an Agilent 6890N GC/5975 MS with a DB5-MS-UI column (30 m × 0.25 mm i.d.) following methods described in Spencer et al. (2010) and Hernes and Benner (2002). Lignin phenol concentrations were measured as the response ratio to *trans*-cinnamic acid, quantified using a five-point

standard curve containing vanillyl (vanillin, acetovanillone, and vanillic acid), syringyl (syringaldehyde, acetosyringone, and syringic acid), and cinnamyl (*p*-coumaric acid and ferulic acid) lignin phenols from 0.5 to 25 ng uL^{-1}. Blank concentrations were <2% of the total lignin concentration.

2.5. FT-ICR MS

Solid phase extracts for FT-ICR MS were ionized with negative electrospray ionization and directly infused into a 21 T FT-ICR MS at a flow rate of 700 nL min^{-1} (Hendrickson et al., 2015; Smith et al., 2018). One hundred consecutive scans were coadded to generate the mass spectrum for each sample with a mass to charge ratio (*m/z*) from 120 to 1,200. Peaks with a signal to noise ratio greater than 6σ RMS baseline noise plus baseline and mass measurement accuracy smaller than 200 ppb were considered for molecular formula assignment (Blakney et al., 2011). Formulae were assignment using EnviroOrg Software (Corilo, 2015) to compounds with molecular formulae containing $C_{1-100}H_{4-200}O_{1-25}N_{0-2}S_{0-1}$. The term compound is used here to describe the underlying molecular compounds comprising DOM identified via FT-ICR MS, however these molecular formulae can represent multiple isomers. Compound classes were defined based on elemental ratios and the modified aromaticity index (AI_{mod}) (Koch & Dittmar, 2006, 2016). Compound classes include highly unsaturated and phenolic ($AI_{mod} < 0.5$, H/C < 1.5), aliphatic (H/C $\geq$ 1.5, $N = 0$), polyphenolic (0.67 > AI_{mod} > 0.5), condensed aromatic ($AI_{mod} \geq 0.67$), peptide-like (H/C $\geq$ 1.5, $N > 0$), and sugar-like (O/C > 0.9) following previously described compound classes (Kellerman et al., 2018; O'Donnell et al., 2016). Relative abundances were calculated as the abundance of each assigned molecular formula scaled to 100%, thus taking into account the different abundances of each molecular formula contribution to the compound classes.

2.6. Flux Calculations and Numerical Analyses

Flux and yield of DOC were calculated for each watershed where a minimum of 12 samples were collected using the USGS developed Load Estimator (LOADEST) program (Runkel et al., 2004). LOADEST provides daily flux estimates based on the relationship between *Q* and concentration and uses daily flux to calculate annual fluxes. For sites with fewer than 12 samples (Atigun and Sagavanirktok Rivers, $n = 11$), discharge and DOC were significantly correlated through the freshet sample period (Figure S1), for these sites a single additional calculated DOC concentration based on discharge was interpolated to reach the minimum requirement of 12 observations to perform flux and yield estimates. Spearman rank correlations were performed on FT-ICR MS data in Python as correlations between relative abundances and landscape and DOM parameters. All correlations were reported as significant at $p < 0.05$ for Spearman rank correlations and linear regressions. Error terms are reported as standard deviation.

3. Results

3.1. Dissolved Organic Carbon Concentrations and Spectral Indices

The concentration of DOC across the six sites ranged from 0.84 to 26.54 mg L^{-1} (mean = 6.85 $\pm$ 6.69 mg L^{-1}, $n = 73$; Figures 2a–2e; Table 2). The Atigun River exhibited the lowest mean DOC concentration (mean = 1.44 $\pm$ 0.57 mg L^{-1}, $n = 11$; Figure 2e; Table 2). The highest DOC concentrations were observed in the Tolovana River, an organic-rich, blackwater river (19.78 $\pm$ 3.95 mg L^{-1}, $n = 13$; Figure 2c; Table 2). Our values from the Tolovana were similar to DOC concentrations measured in 2002 (13.99 mg L^{-1}) and 2005–2006 (8.7–24.4 mg L^{-1}) (O'Donnell et al., 2010; Spencer et al., 2008). Peak DOC concentrations generally corresponded with the freshet and declined throughout the remainder of the sampled ice-free season. All sites except Tolovana experienced high *Q* events later in the ice-free season (Figure 2). At sites where the late high *Q* event was sampled (Salcha and Chena), relatively high DOC concentrations were observed (Figures 2a–2c). The DOC minima observed in the Chena and Salcha Rivers during low *Q* (2.72 and 3.24 mg L^{-1}, respectively; Figures 2a and 2b) were similar to those observed in a previous study of winter baseflow DOC concentrations (2.3 and 2.4 mg L^{-1}, respectively) (O'Donnell et al., 2012).

Absorbance parameters included a_{254} and a_{350}, $S_{275-295}$ and $S_{350-400}$, S_R, and SUVA$_{254}$. Across the six sites a_{254} ranged from 4.8 to 233.3 m^{-1} (mean = 58.9 $\pm$ 61.9 m^{-1}, $n = 73$; Table 2) and means ranged from
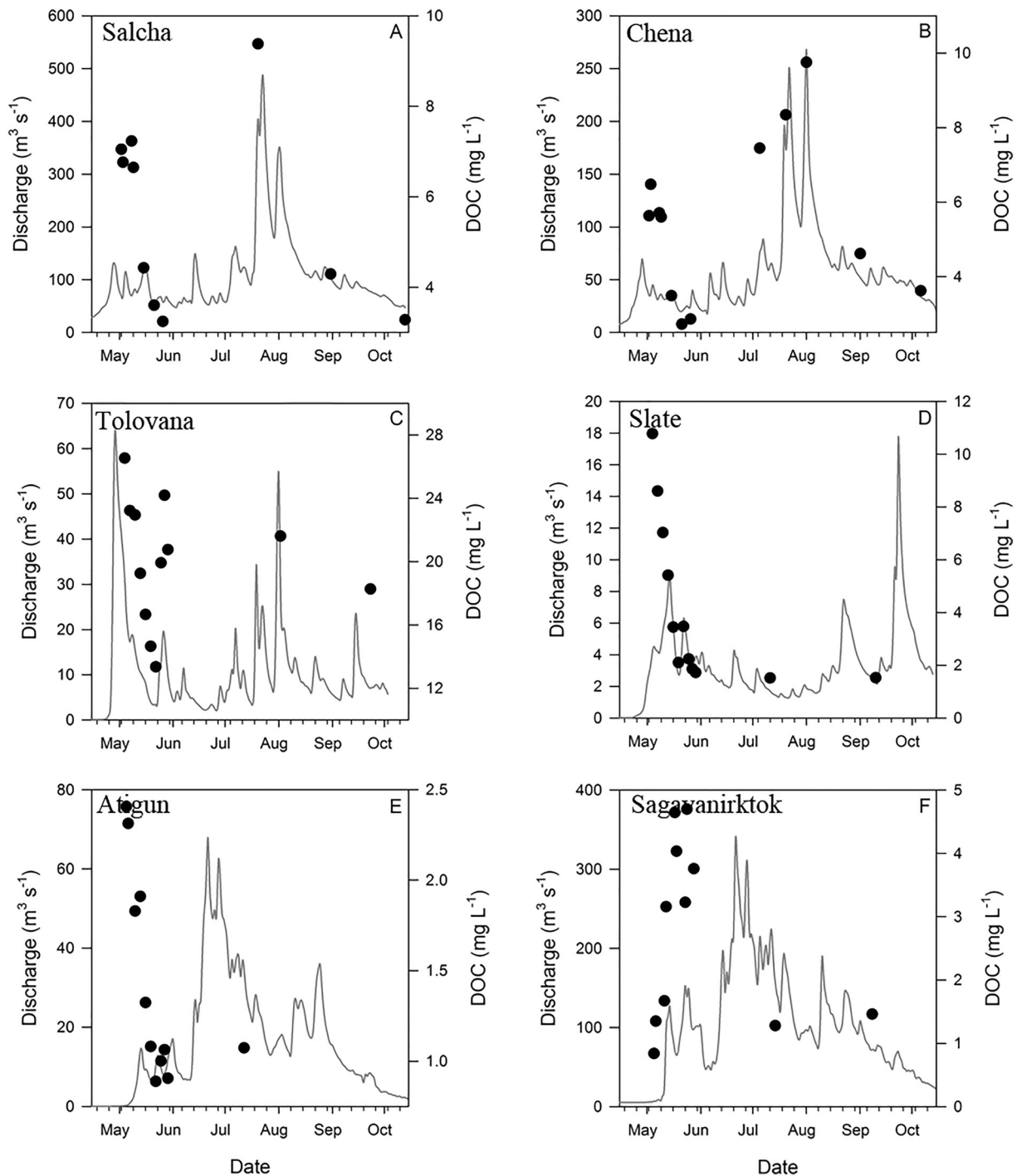
Figure 2. Discharge (gray line) and DOC concentrations (black dots) at each site from April 15 to October 15, 2016. A- Salcha, B- Chena, C- Tolovana, D- Slate, E- Atigun, F- Sagavanirktok.

21.6 $\pm$ 14.1 m^{-1} in the Sagavanirktok River to 177.2 $\pm$ 38.8 m^{-1} in the Tolovana River. The mean a_{350} across all sites was 16.3 $\pm$ 17.2 m^{-1} (1.0–65.0 m^{-1}, $n = 73$; Table 2). Similar to DOC, the lowest a_{350} was observed in the Atigun River (2.2 $\pm$ 1.1 m^{-1}) and the highest in the Tolovana River (48.8 $\pm$ 11.3 m^{-1}; Table 2). The lowest a_{254} and a_{350} values were observed in the sites underlain by continuous permafrost (Atigun and Sagavanirktok Rivers) compared to the highest averages observed in the Tolovana River with the deepest active layer (Table 2). Spectral slope ranges have previously been related to DOM source and aromaticity

Table 2
Mean, Minimum (Min), Maximum (Max), and Standard Deviation (SD) for Dissolved Organic Carbon (DOC) Concentration and Optical FT-ICR MS Parameters for Each Site and All Sites Combined

Site		DOC (mg L⁻¹)	a_{254} (m⁻¹)	a_{350} (m⁻¹)	$S_{275-295}$ (μm⁻¹)	$S_{350-400}$ (μm⁻¹)	S_R	SUVA$_{254}$ (L mg C⁻¹ m⁻¹)	FI	Number of assigned molecular formulae	AI$_{mod}$	Highly unsaturated and phenolic (%RA)	Polyphenolic (%RA)	Condensed aromatic (%RA)	Aliphatic (%RA)	Peptide-like (%RA)	Sugar-like (%RA)
Salcha	Mean	5.90	50.7	14.2	13.78	16.10	0.86	3.6	1.60	8,045	0.33	83.2	11.1	2.7	2.4	0.0	0.6
$n = 12$	Min	3.24	19.1	4.3	12.08	13.81	0.76	2.5	1.53	6,457	0.30	77.7	7.3	1.1	1.7	0.0	0.4
	Max	9.38	80.0	23.3	15.82	17.81	0.91	4.1	1.63	9,056	0.35	89.4	14.6	4.2	2.8	0.1	0.9
	SD	2.05	21.4	6.7	1.32	1.43	0.05	0.5	0.03	622	0.01	3.3	2.1	0.9	0.4	0.0	0.2
Chena	Mean	5.47	44.4	11.9	14.15	16.59	0.85	3.4	1.60	7,812	0.33	83.7	11.1	2.4	2.0	0.1	0.8
$n = 14$	Min	2.72	17.8	4.1	12.39	15.12	0.77	2.5	1.52	4,795	0.31	80.9	8.2	1.4	1.5	0.0	0.4
	Max	9.75	83.7	22.8	15.92	18.12	0.91	3.9	1.63	9,180	0.34	88.2	12.9	3.2	2.6	0.4	1.0
	SD	2.05	19.8	5.7	1.10	0.93	0.04	0.5	0.04	1,125	0.01	2.6	1.7	0.7	0.3	0.1	0.2
Tolovana	Mean	19.78	177.2	48.8	13.46	16.73	0.80	3.9	1.59	8,417	0.34	80.9	12.5	3.3	2.2	0.1	1.1
$n = 13$	Min	13.35	112.2	29.2	13.04	15.63	0.77	3.5	1.49	7,029	0.32	76.5	10.7	2.3	1.5	0.0	0.9
	Max	26.54	233.3	65.0	14.29	18.19	0.84	4.1	1.67	9,586	0.35	84.5	14.2	5.0	3.2	0.1	1.2
	SD	3.95	38.8	11.3	0.47	0.71	0.02	0.2	0.06	789	0.01	2.2	1.1	0.8	0.4	0.0	0.1
Slate	Mean	4.14	36.0	9.9	13.84	17.08	0.81	3.5	1.59	8,176	0.32	82.9	10.6	2.8	3.2	0.1	0.5
$n = 12$	Min	1.52	8.5	1.9	12.54	15.99	0.75	2.4	1.53	6,989	0.29	78.1	6.3	1.1	2.5	0.0	0.3
	Max	10.78	94.6	26.8	15.76	19.03	0.87	4.3	1.67	9,440	0.34	89.7	13.9	4.2	3.7	0.2	0.8
	SD	3.13	30.1	8.8	1.05	0.97	0.04	0.6	0.05	708	0.02	4.0	2.5	1.1	0.4	0.0	0.2
Atigun	Mean	1.44	8.6	2.2	16.20	16.56	1.02	2.6	1.55	10,244	0.31	81.0	10.7	2.8	4.7	0.4	0.5
$n = 11$	Min	0.89	5.1	1.0	13.56	9.74	0.76	2.1	1.51	9,617	0.30	77.3	9.4	2.2	3.9	0.1	0.2
	Max	2.41	14.4	4.3	17.77	21.17	1.58	3.0	1.59	10,872	0.33	83.6	12.8	3.9	6.1	1.3	0.7
	SD	0.57	3.5	1.1	1.22	3.45	0.22	0.3	0.03	416	0.01	2.2	1.1	0.5	0.8	0.4	0.2
Sagavanirktok	Mean	2.74	21.6	6.5	14.10	11.72	1.42	3.1	1.55	8,500	0.33	79.3	12.7	3.6	3.6	0.1	0.7
$n = 11$	Min	0.84	4.8	1.5	11.71	5.48	0.84	2.3	1.49	7,379	0.29	74.3	7.2	1.2	2.7	0.0	0.2
	Max	4.70	42.0	12.6	16.36	16.47	2.86	3.9	1.65	9,784	0.36	88.5	16.2	5.3	5.5	0.3	1.0
	SD	1.45	14.1	4.1	1.56	4.08	0.75	0.6	0.05	809	0.03	4.7	3.2	1.4	1.0	0.1	0.3
All sites	Mean	6.85	58.9	16.3	14.22	15.88	0.95	3.4	1.58	8,488	0.33	81.9	11.4	2.9	2.9	0.1	0.7
$n = 73$	Min	0.84	4.8	1.0	11.71	5.48	0.75	2.1	1.49	4,795	0.29	74.3	6.3	1.1	1.5	0.0	0.2
	Max	26.54	233.3	65.0	17.77	21.17	2.86	4.3	1.67	10,872	0.36	89.7	16.2	5.3	6.1	1.3	1.2
	SD	6.69	61.9	17.2	1.41	2.80	0.36	0.6	0.05	1,092	0.02	3.5	2.2	1.0	1.1	0.2	0.3

(Helms et al., 2008). The $S_{275-295}$ varied from 11.71 to 17.77 μm^{-1} (mean = 14.22 ± 1.41 μm^{-1}, n = 73). The shallowest mean $S_{275-295}$ was observed in the Tolovana River (13.46 ± 0.47 μm^{-1}) and the steepest mean in the Atigun River (16.20 ± 1.22 μm^{-1}) (Table 2). The mean $S_{275-295}$ observed in this study was similar to values previously reported for the Yukon River during peak Q (12 μm^{-1}) (Kellerman et al., 2018). Across all sites, the average $S_{350-400}$ was 15.88 ± 2.80 μm^{-1} (n = 73) and ranged from 5.48 μm^{-1} prior to the freshet in the Sagavanirktok River (mean = 11.72 ± 4.08 μm^{-1}) to 21.17 μm^{-1} during the freshet in the Atigun River (mean = 16.56 ± 2.40 μm^{-1}; Table 2). The S_R is related to the molecular weight and aromatic content of DOM (Helms et al., 2008), and exhibited a mean of 0.95 ± 0.36 across all the sites, and ranged from 0.75 during the summer in the Slate (mean = 0.81 ± 0.04) to 2.86 prior to the freshet in the Sagavanirktok River (mean = 1.42 ± 0.75, Table 2, Table S2).

SUVA$_{254}$ has been linked to DOM aromaticity with more aromatic samples exhibiting higher SUVA$_{254}$ values (Weishaar et al., 2003). SUVA$_{254}$ ranged from 2.1 L mg C^{-1} m^{-1} in the Atigun River to 4.3 L mg C^{-1} m^{-1} in Slate Creek at the peak of the freshet. Across all sites, the mean SUVA$_{254}$ value was 3.4 ± 0.6 L mg C^{-1} m^{-1}. The range and mean of SUVA$_{254}$ was similar to those observed by Spencer et al. (2008) for streams and rivers in the Yukon River Basin (1.3–4.5 L mg C^{-1} m^{-1}, mean = 3.1 L mg C^{-1} m^{-1}). Atigun River exhibited the lowest mean SUVA$_{254}$ (2.6 ± 0.3 L mg C^{-1} m^{-1}) and the Tolovana River exhibited the highest mean SUVA$_{254}$ values (3.9 ± 0.2 L mg C^{-1} m^{-1}; Table 2). Minimum SUVA$_{254}$ values observed here were similar to a previously reported under-ice SUVA$_{254}$ value from the Salcha River (2.4 L mg C^{-1} m^{-1}) (O'Donnell et al., 2012). The mean SUVA$_{254}$ observed in the Atigun River was similar to under-ice SUVA$_{254}$ reported for streams and rivers in interior Alaska (2.5–3.2 L mg C^{-1} m^{-1}) (O'Donnell et al., 2010). Similar to a_{254} and a_{350}, SUVA$_{254}$ was lowest in the site with shallow ALT and low vegetation cover (Atigun; Table 1) and highest in the site with the deepest ALT (Tolovana; Table 1).

The FI is related to DOM composition and source, with values typically ranging from ~1.4 in terrestrially dominated, aromatic rich blackwater systems to ~1.9 for microbially derived aromatic poor DOM (Cory & McKnight, 2005; McKnight et al., 2001). Our values encompass the range of values previously observed for similar sites in interior Alaska (1.5–1.8) (Harms et al., 2016), ranging from 1.49 in the Sagavanirktok and Tolovana Rivers during the freshet to 1.67 in Slate Creek during the fall when Q was low (mean = 1.58 ± 0.05, n = 73; Table 2). The mean FI among all sites exhibited little variation (1.55–1.60). The lowest mean FI was observed in the Atigun and Sagavanirktok Rivers (1.55 ± 0.03, 1.55 ± 0.05, respectively), both of which are underlain by continuous permafrost. The highest FI was observed at the most southern sites, the Salcha and Chena Rivers (1.60 ± 0.03, 1.60 ± 0.04, respectively), which are underlain by discontinuous permafrost.

3.2. Lignin Phenol Biomarkers

Lignin is exclusively produced by vascular plants and provides a robust tracer of terrestrially sourced DOM in aquatic systems (Hedges & Mann, 1979; Hernes & Benner,, 2003). Lignin phenols were measured on a subset of samples (n = 29) due to the large sample volumes required and the analytically intensive and expensive method. Samples were collected for lignin every second site visit to each site ensuring that samples spanned a range of discharge during the freshet period. Lignin concentration was calculated as the sum of the eight lignin phenols (Σ_8) and ranged from 1.71 μg L^{-1} in the Atigun River to 132.16 μg L^{-1} in the Tolovana River. The mean Σ_8 across all sites was 20.81 ± 31.47 μg L^{-1} (n = 29; Table 3). The range and mean Σ_8 was similar to previous measurements in rivers and streams in interior Alaska (0.8–124.4 μg L^{-1}, mean = 27.5 μg L^{-1}, n = 29) (Spencer et al., 2008). Generally, Σ_8 increased through the peak of the freshet and decreased following freshet (Table S3).

The relative contribution of vascular plant material to the bulk DOM pool was assessed using the carbon normalized lignin yield of the eight lignin phenols (Λ_8). Values for Λ_8 ranged from 0.10 mg (100 mg OC)$^{-1}$ in the Chena River following the freshet, to 0.50 mg (100 mg OC)$^{-1}$ in Slate Creek and the Tolovana River also around freshet (Figure 3; Table 3). The mean Λ_8 across sites was 0.26 ± 0.12 mg (100 mg OC)$^{-1}$ (n = 29; Table 3). The Chena and Salcha Rivers exhibited the lowest mean Λ_8 (mean = 0.15 ± 0.02 and 0.15 ± 0.04 mg (100 mg OC)$^{-1}$, respectively; Figures 3a and 3b) and the highest Λ_8 was observed in the Tolovana River (mean = 0.39 ± 0.08 mg (100 mg OC)$^{-1}$; Figure 3c; Table 3). The Λ_8 typically peaked with Q; this is most pronounced in the Tolovana River where sampling began just following freshet and Λ_8 declined from 0.50

Table 3

Lignin Parameter Statistics (Mean, Minimum [Min], Maximum [Max], and Standard Deviation [SD]) Including Lignin Concentration (Σ_8) and Yield (Λ_8) and the Ratios of the Cinnamyl to Vanillyl (C/V) and Syringyl to Vanillyl (S/V) for Each Site and the Combined Statistics

Site		Σ_8 (μg L^{-1})	Λ_8 (mg (100 mg OC)$^{-1}$)	C/V	S/V
Salcha	Mean	7.94	0.15	0.35	0.61
$n = 5$	Min	3.96	0.12	0.20	0.59
	Max	11.92	0.17	0.51	0.68
	SD	3.71	0.02	0.13	0.04
Chena	Mean	6.52	0.15	0.40	0.55
$n = 5$	Min	2.80	0.10	0.18	0.53
	Max	11.00	0.20	0.66	0.58
	SD	3.77	0.04	0.21	0.02
Tolovana	Mean	89.25	0.39	0.21	0.52
$n = 4$	Min	50.98	0.31	0.17	0.48
	Max	132.16	0.50	0.23	0.55
	SD	33.53	0.08	0.03	0.03
Slate	Mean	21.94	0.36	0.28	0.76
$n = 5$	Min	3.08	0.17	0.19	0.67
	Max	48.97	0.50	0.54	0.92
	SD	18.58	0.15	0.15	0.09
Atigun	Mean	3.53	0.22	0.81	0.97
$n = 5$	Min	1.71	0.18	0.56	0.72
	Max	6.41	0.27	0.91	1.26
	SD	2.01	0.04	0.14	0.20
Sagavanirktok	Mean	9.39	0.29	0.89	1.22
$n = 5$	Min	2.32	0.23	0.63	1.00
	Max	16.81	0.36	1.14	1.34
	SD	5.16	0.05	0.19	0.13
All sites	Mean	20.81	0.26	0.50	0.78
$n = 29$	Min	1.71	0.10	0.17	0.48
	Max	132.16	0.50	1.14	1.34
	SD	31.47	0.12	0.30	0.27

to 0.31 mg (100 mg OC)$^{-1}$ and then increased with discharge in late May 2016 (0.34 mg (100 mg OC)$^{-1}$) (Table S3).

The ratios of the lignin phenols are used to distinguish between plant tissue sources (Hedges & Mann, 1979; Spencer et al., 2008) and may be related to DOM phase changes (Hernes et al., 2007). The ratio of the cinnamyl to vanillyl phenols (C/V) and syringyl to vanillyl phenols (S/V) varies by plant type and distinguishes between woody and nonwoody sources and angiosperm versus gymnosperm sources of lignin (Hedges & Mann, 1979). In Arctic and boreal regions these ratios can be altered by the presence of non-vascular vegetation such as mosses that are abundant in these regions (Amon et al., 2012; Moingt et al., 2016; Williams et al., 1998). Across all sites, C/V ranged from 0.17 to 1.14 (mean = 0.50 ± 0.30, $n = 29$; Table 3; Figure 4), representing values that are a mix of nonwoody and woody tissues. The S/V ratios ranged from 0.48 to 1.34 (mean = 0.78 ± 0.27, $n = 29$; Table 3; Figure 4) and were representative of a mix of gymnosperm to predominantly angiosperm derived lignin sources (Spencer et al., 2008). The Atigun and Sagavanirktok Rivers, sites north of the tree line on the North Slope, exhibited ratios typical of nonwoody angiosperm tissue, while all other sites comprised a mixture of sources (Figure 4). The ratios of C/V and S/V were higher than previously measured in the Yukon River Basin (0.15–0.72 and 0.46–0.80, respectively), which did not include sites north of the tree line dominated by tundra vegetation (Spencer et al., 2008). Lichen and moss cover was significantly positively correlated to both C/V and S/V ratios ($r^2 = 0.77$ and 0.98, respectively, $p < 0.05$), while forest cover was negatively correlated with S/V ratio ($r^2 = 0.78$, $p < 0.05$), and grass or shrubland cover was negatively correlated with C/V ratio ($r^2 = 0.73$, $p < 0.05$; Tables S1 and S3).

3.3. Molecular Composition

Compositional changes to DOM were evaluated via FT-ICR MS across the seasonal and latitudinal gradient. The number of molecular formulae assigned ranged from 4,795 in the Chena River to 10,872 in the Atigun River (mean = $8,488 \pm 1,092$, $n = 73$; Table 2), and 4,133 molecular formulae were common to all samples. Aromaticity was evaluated using AI$_{mod}$ with higher values associated with more terrestrially derived DOM sources (Koch & Dittmar, 2006). The mean AI$_{mod}$ was 0.33 ± 0.02 (0.29–0.36, $n = 73$; Table S2), similar to values observed from the Northern Dvina River, an Arctic river dominated by vascular plant inputs (mean = 0.35) (Johnston et al., 2018). The lowest mean AI$_{mod}$ was observed in the Atigun River (0.31 ± 0.01), which also exhibited the lowest

mean SUVA$_{254}$. The maximum mean AI$_{mod}$ was observed in the Tolovana River (0.34 ± 0.01), where maxima mean Λ_8 and SUVA$_{254}$ were also observed (Tables 2 and 3; Figure 3).

Compound classes identified via FT-ICR MS are related to DOM source and reactivity (D'Andrilli et al., 2015; Kellerman et al., 2018; O'Donnell et al., 2016). Here we compare the relative abundances of these broad compound classes with the caveat that some compound classes ionize more efficiently compared to others (Kujawinski, 2002). The highly unsaturated and phenolic compound class accounted for a majority of the relative abundance of assigned molecular formulae ($81.9 \pm 3.5\%$, $n = 73$; Figure 5). Polyphenolics are predominantly derived from terrestrially derived DOM, such as lignin and tannins (Kellerman et al., 2014). The relative abundance of polyphenolics ranged from 6.3% in Slate Creek during the fall to 16.2% in the Sagavanirktok River at the peak of freshet (mean = $11.4 \pm 2.2\%$, $n = 73$; Figure 5; Table 2). The relative abundance of polyphenolics increased with discharge in all sites except the Atigun River (Table S2).
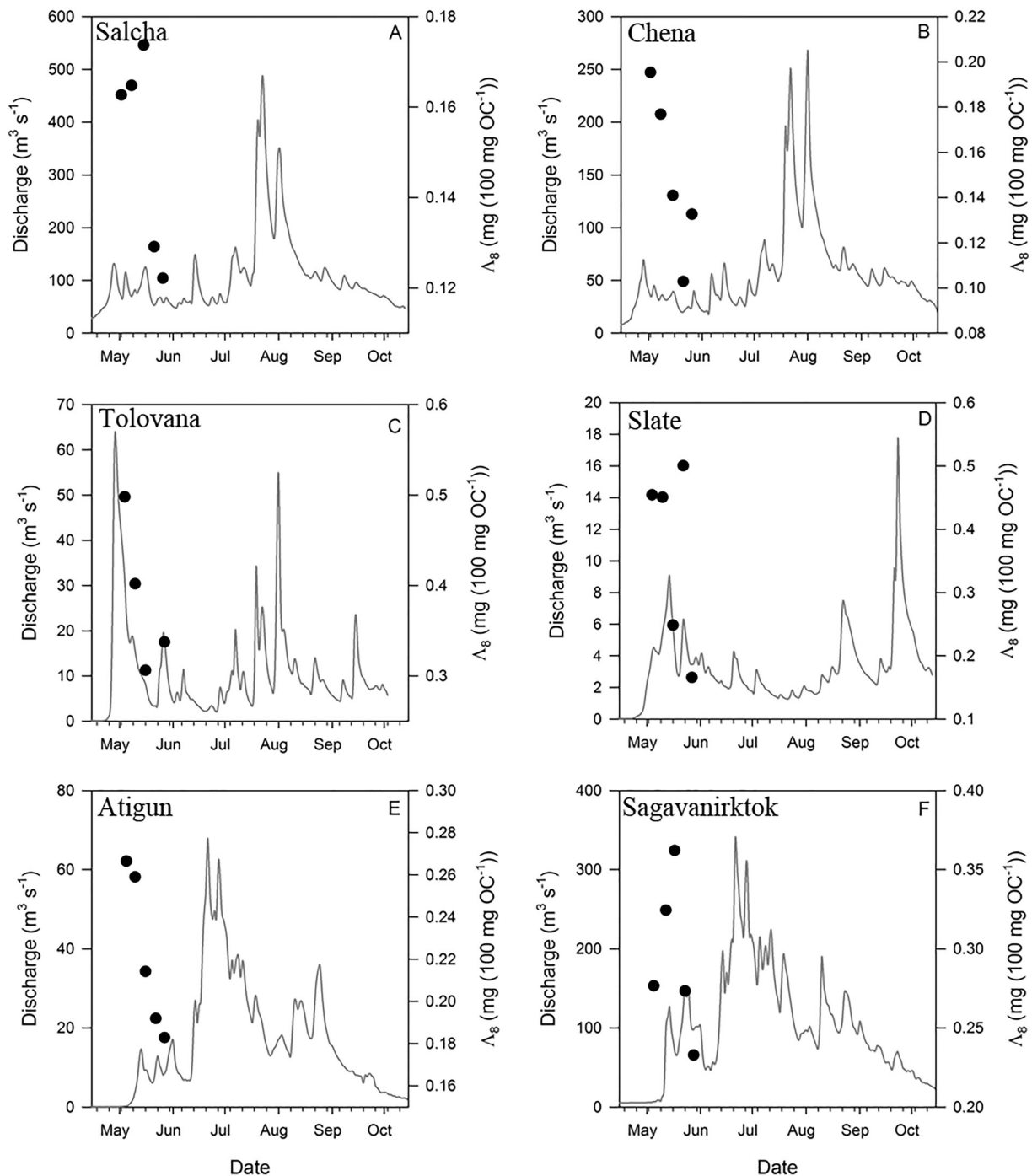
Figure 3. Carbon normalized lignin yield (black dots) plotted with the hydrograph (gray line) for each site in 2016. A- Salcha, B- Chena, C- Tolovana, D- Slate, E- Atigun, F- Sagavanirktok.

Condensed aromatics are related to terrestrial DOM derived from incomplete combustion of organic matter and non-pyrogenic degradation of terrestrial DOM (Waggoner et al., 2015). The relative abundance of condensed aromatics ranged from 1.1% during the fall in Slate Creek to 5.3% in the Sagavanirktok River at the peak of freshet (mean = 2.9 ± 1.0%). Condensed aromatics increased with increasing discharge through the freshet (Table S2). The aliphatic, peptide-like, and sugar-like compound classes are typically associated with more biolabile DOM derived from fresh sources such as plant leachates, and also well-preserved organic matter such as permafrost (D'Andrilli et al., 2015; Spencer et al., 2015; Textor et al., 2019). The aliphatic
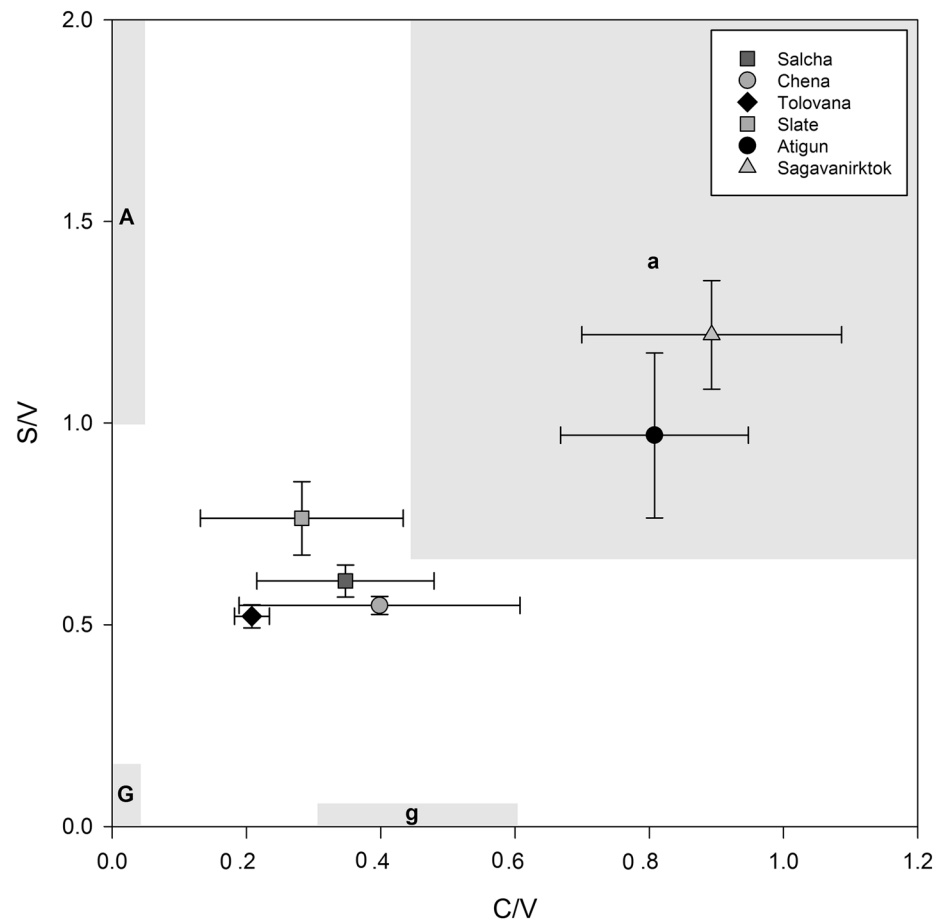
Figure 4. Mean and standard deviation of lignin phenol ratios of cinnamyl to vanillyl (C/V) and syringyl to vanillyl (S/V) for each site. Sites include: Salcha (dark gray square), Chena (gray circle), Tolovana (black diamond), Slate (gray square), Atigun (black circle), and Sagavanirktok (light gray triangle). Boundaries for plant tissue types from Spencer et al. (2008) include woody gymnosperm (G), nonwoody gymnosperm (g), woody angiosperm (A), and nonwoody angiosperm (a).

compound classes ranged from 1.5% to 6.1% (mean $= 2.9 \pm 1.1\%$, $n = 73$; Figure 5; Table 2) and exhibited the highest mean relative abundance in the Atigun River (mean $= 4.7 \pm 0.8\%$) and lowest in the Chena River ($2.0 \pm 0.3\%$). Across all sites, the combined relative abundance of sugar-like and peptide-like compound classes did not exceed 2%. Peptide-like relative abundance was highest in the Atigun River ($0.4 \pm 0.4\%$; Figure 5; Table S2) compared to the mean among all the sites ($0.1 \pm 0.2\%$; Table 2) and has been found to be a minor contributor to DOM composition across the aquatic continuum (Kellerman et al., 2018). Sugar-like compounds were low across all sites ($0.7 \pm 0.3\%$; Figure 5; Table 2) and reached a maximum following peak of the freshet (1.2%; Table S2).

3.4. Fluxes and Yields of DOC

The DOC flux ranged from 0.4 Gg yr^{-1} from Slate Creek to 18.2 Gg yr^{-1} from the Salcha River (Table 1) and was significantly and positively correlated with watershed area ($r^2 = 0.68$, $p < 0.05$). The DOC yield, DOC flux normalized to catchment area, ranged from 1.4 g m^{-2} yr^{-1} in the Atigun watershed to 9.4 g m^{-2} yr^{-1} from the Tolovana watershed (Table 1). Watershed relief and mean annual water yield were inversely related to DOC yield ($r^2 = 0.69$, $p < 0.01$; $r^2 = 0.80$, $p < 0.01$, respectively). The lowest yields were observed from the sites with the steepest average relief and highest mean annual water yield. The DOC yields observed in this study were comparable to DOC fluxes and yields from similarly sized rivers and streams in the Yukon River Basin (Frederick et al., 2012).
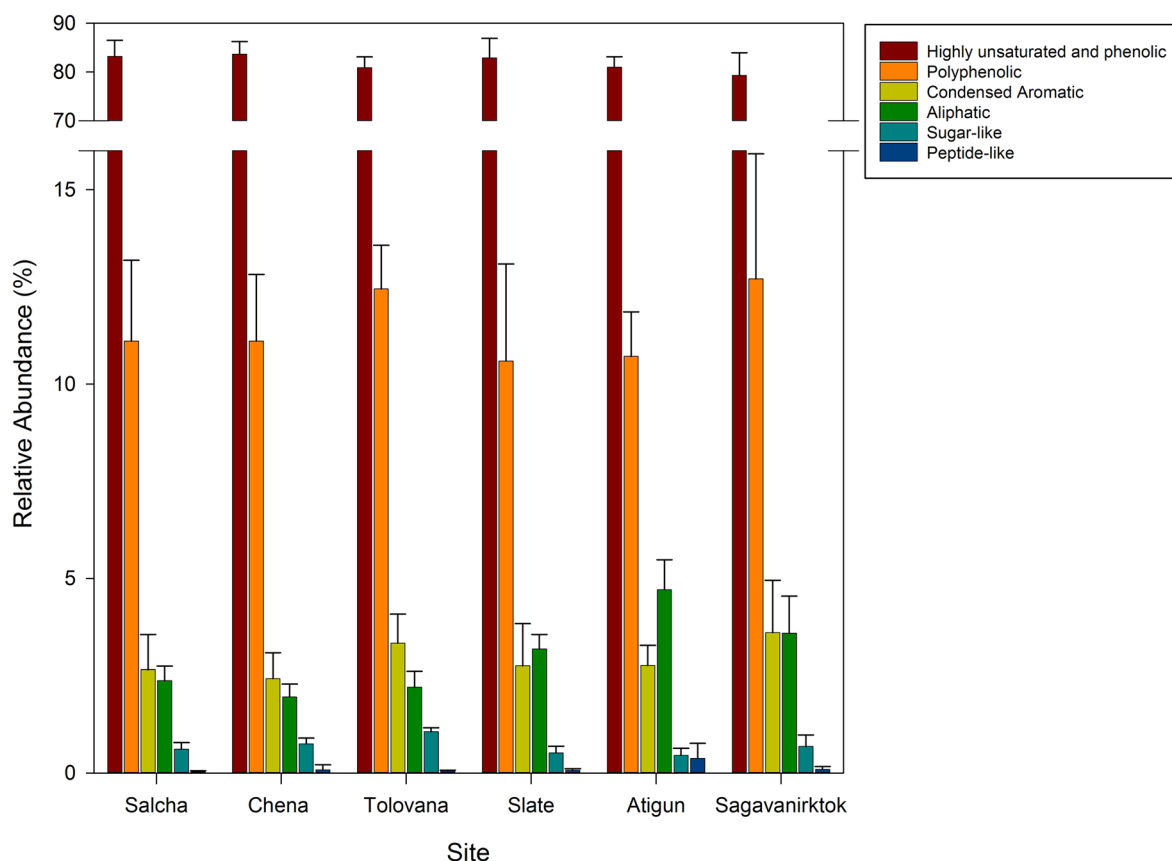
Figure 5. Mean relative abundance and standard deviation of compound classes at each sample site. Compound classes include: highly unsaturated and phenolic (red), polyphenolic (orange), condensed aromatic (yellow), aliphatic (green), sugar-like (teal), and peptide-like (blue).

4. Discussion

4.1. Seasonal Drivers of DOM Composition

Arctic rivers are characterized by strong shifts in seasonal inputs, particularly from the spring snowmelt (Holmes et al., 2012; Mann et al., 2016; O'Donnell et al., 2010). Discharge and DOC concentration were significantly positively correlated only in sites underlain by discontinuous permafrost (Salcha, Chena, and Tolovana Rivers: $r^2 = 0.41$, 0.67, and 0.71, respectively, $p < 0.05$), highlighting a relatively linear relationship between Q and DOC export in these watersheds (Figures 2a–2c; Figure S1). At Slate Creek, a small watershed underlain by continuous permafrost, maximum DOC concentrations in 2016 preceded the freshet (Figure 2d; Table S2), likely due to the initial mobilization of DOM followed by dilution with surface runoff in this less vegetated watershed (Mann et al., 2012).

Our sampling captured the onset of the spring freshet in the Atigun and Sagavanirktok Rivers, but we did not sample at high resolution through peak Q, which occurred in June. In the Atigun River, DOC concentrations decreased through the freshet, but this may be due to the lack of a single defined Q peak during freshet at the Atigun River during 2016. A decrease in DOC concentration at elevated Q in the spring could occur if terrestrial DOM from surface runoff was mobilized during the initial snowmelt in this largely unvegetated and steep watershed. DOM is subsequently diluted or the depletion of leachable source materials as evidenced by decreasing lignin yields throughout the snowmelt period (Figures 2e and 3e; Table 1). The peak in DOC concentrations prior to the freshet is consistent with previous observations on the Kolyma River, a large Arctic river completely underlain by continuous permafrost (Amon et al., 2012; Mann et al., 2012). The Sagavanirktok River did not exhibit a clear trend with DOC and Q, but, unlike the Atigun River, DOC concentrations did generally increase at elevated Q (Figure 2f; Table S2).
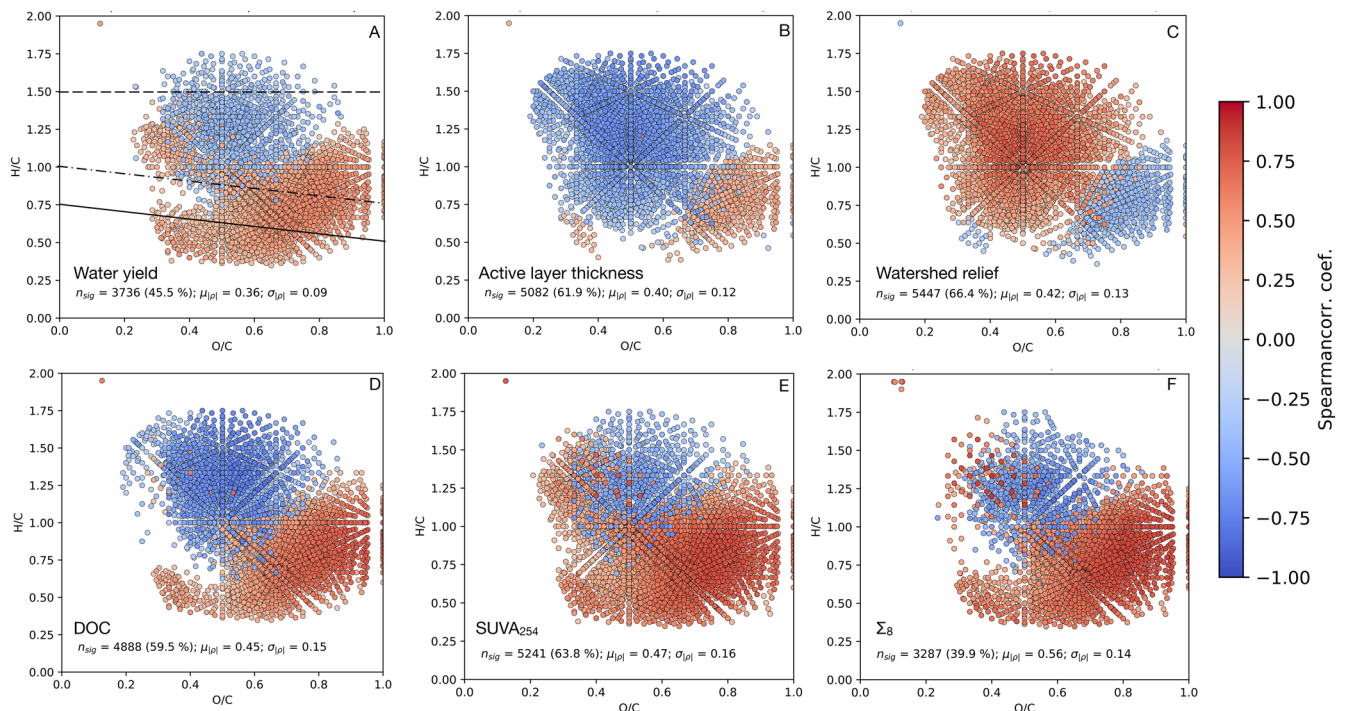
Figure 6. Spearman correlation of molecular formulae present in at least 75% of samples with landscape and DOM parameters across all sites for (a) water yield, (b) active layer thickness, (c) watershed relief slope, (d) DOC concentration, (e) SUVA$_{254}$, and (f) lignin concentration. All correlations shown were significant at $p < 0.05$ and molecular formulae used for correlations were present in at least 50% of all samples. Correlation statistics are reported for each parameter including the number of molecular formulae with significant correlations (percent of total molecular formulae assigned), the mean ($\mu_{|\rho|}$) and standard deviation ($\sigma_{|\rho|}$) are reported for the absolute value of ρ_s, the Spearman rank correlation coefficient. In panel A the dashed, dashed/dot, and solid lines separate (from top to bottom) aliphatic, highly unsaturated and phenolic, polyphenolic, and condensed aromatic compound classes.

Freshet and periods of high Q corresponded with greater terrestrial DOM contribution, assessed via SUVA$_{254}$ and Λ_8 (Figures 3a–3f; Tables S2 and S3). Other optical DOM indices including $S_{275–295}$, S_R, and FI were correlated to Q at individual sites, but not across sites. Except in the Atigun, S_R was negatively correlated to Q at all sites, indicating that the relative contribution of higher molecular weight and more aromatic DOM associated with terrestrial sources increases with Q (Amon et al., 2012; Helms et al., 2008; Kaiser et al., 2017; Mann et al., 2012). Similarly, FI decreased with Q in the Yukon River Basin sites, demonstrating the increase in aromatic DOM during high Q events (Mann et al., 2012; O'Donnell et al., 2012). In the Atigun and Saga-vanirktok Rivers, FI is positively correlated with Q, indicating an increase in less-aromatic sources of DOM with increasing Q north of the tree line.

The daily water yield (Table S2), was strongly positively correlated with high O/C polyphenolic and condensed aromatic formulae identified via FT-ICR MS (Figure 6a). This is similar to increases in terrestrial DOM contribution observed in major Arctic rivers at high Q (Raymond et al., 2007; Spencer et al., 2009; Striegl et al., 2007). During low Q, when surface runoff is low and greater proportions of groundwater contribute to streamflow, higher relative abundances of aliphatic molecular formulae were observed, concurrent with lower DOC and lignin concentrations and lower SUVA$_{254}$ values (Figures 2a–2f and 6a; Table S2). This suggests that predicted increases in groundwater Q to these rivers as permafrost thaws (Koch et al., 2014; Striegl et al., 2005; Walvoord & Striegl, 2007), may be accompanied with an associated shift toward DOM that is less aromatic as supra-permafrost flow interacts with deeper mineral soil layers (Kaiser & Guggenberger, 2000) and there is enhanced contribution from sub-permafrost groundwater (Figure 6a). These patterns show that hydrologic shifts in the seasonality and sources of Q have direct impacts to fluvial DOM composition in the warming Arctic, and that along the latitudinal gradient southern sites underlain by discontinuous permafrost that are more vulnerable to change including earlier snowmelt, longer periods of active layer thawing, and associated hydrologic changes may be indicators of expected changes in more northern sites.

4.2. DOM Composition Across a Landscape Gradient

Catchment slope and ALT play a significant role in controlling DOM composition in Arctic rivers (Harms et al., 2016; Koch et al., 2013; O'Donnell et al., 2010). In this study, ALT exerts a control on DOM composition, both seasonally and at the landscape scale. Sites with deeper ALT (i.e., the Tolovana River) exhibited lower relative abundances of aliphatic molecular formulae compared to sites with shallower ALT (Figure 5). The maximum ALT was positively correlated with mean $SUVA_{254}$ at each site ($r^2 = 0.96$, $p < 0.01$) and with molecular formulae corresponding to polyphenolic and condensed aromatic compound classes (Figure 6b). This observation could be related to the warmer soil temperatures associated with deeper ALT and has previously been observed to be associated with increased $SUVA_{254}$ (O'Donnell et al., 2016) and the varying landscape characteristics of these watersheds (Table 1). As the active layer deepens and temperatures warm, the interaction of supra-permafrost flow with soil organic matter may increase the export of aromatic, terrestrial DOM (O'Donnell et al., 2016). Additionally, as sites experiencing increased ALT and temperatures, vegetation community composition may shift toward more woody vegetation, further altering the DOM composition (Abbott et al., 2016; Neff & Hooper, 2002; Pearson et al., 2013).

Vegetation cover (Table S1, Carey et al., 2020) was correlated to DOM composition, particularly with regards to lignin biomarkers. The lowest lignin concentration was observed in the Atigun River, a mountainous watershed that is 54% barren (Tables 3 and S1). Lignin phenol ratios also showed evidence of landscape controls, as we observed greater inputs from nonwoody angiosperm tissue to the bulk lignin pool in sites north of the tree line dominated by mosses and lichens (Figure 4; Table S1). This result suggests that as the tree line moves northward, there may be a shift in lignin composition and increase in lignin concentration in more northern Arctic rivers as forest productivity changes (ACIA, 2004; Kane et al., 2005, 2006). In the steep, northern Atigun and Sagavanirktok watersheds with shallow ALT, the relative abundance of aliphatic molecular formulae was higher compared to other watersheds (Figure 5), likely a result of input of DOM sourced from lichens and mosses as past studies have shown these to be enriched in aliphatic molecular formulae upon leaching (Johnston et al., 2019). Rivers with steeper watershed relief exhibited higher relative abundances of DOM with lower O/C and less aromatic molecular formulae compared to sites with shallower watershed relief (Figure 6c). These results suggest that rivers north of the tree line that drain catchments containing non-vascular sources of vegetation, likely export a larger fraction of biolabile material, as aliphatics have been shown to be a good predictor of biolability (Spencer et al., 2015; Textor et al., 2019). Soil organic carbon shifts along latitudinal gradients have shown that warmer soils contain lower fractions of relatively biolabile DOM (Kane et al., 2005), suggesting that these DOM differences could in part be linked to landscape ecology. As woody vegetation expands northward, particularly increased distribution of shrubby vegetation, the ecological succession in this region with projected climate change will have ramifications for stream biogeochemistry including the composition of vascular plant derived DOM.

4.3. Optical Proxies for DOC Concentration and DOM Composition

The use of CDOM as a proxy for DOC concentration and DOM composition allows the use of in situ sensors or remote sensing to assess DOM across broad temporal and spatial scales, respectively (Griffin et al., 2018; Pellerin et al., 2012; Spencer et al., 2007). In this study, a_{350} correlated with DOC concentration across all sites ($r^2 = 0.99$, $p < 0.01$; Figure 7a) and scales with Q. These relationships were similar to those observed for streams and rivers in the Yukon River Basin by Spencer et al. (2008), with slightly higher CDOM per unit DOC compared to the previous relationship (Figure 7a). The similarity between the two models suggests that CDOM is a robust predictor of DOC concentration in rivers from the interior to the North Slope of Alaska.

DOC concentration was positively correlated with the relative abundance of polyphenolic and condensed aromatic DOM and negatively correlated with aliphatic DOM (Figure 6d), consistent with the relationships between optical parameters and DOC concentration (Figures 2a–2f; Table S2). Optical parameters were strongly correlated to DOM composition: $SUVA_{254}$ and AI_{mod} were significantly related ($r^2 = 0.67$, $p < 0.05$), as previously observed (Johnston et al., 2018; Kellerman et al., 2018). Molecular formulae that were significantly associated with $SUVA_{254}$ were largely aromatic (Figure 6e), further confirming the utility of $SUVA_{254}$ as a proxy for aromaticity. Additionally, during spring freshet there was an increase in the relative abundance of aliphatic molecular formulae, this higher relative abundance of aliphatic formulae during freshet
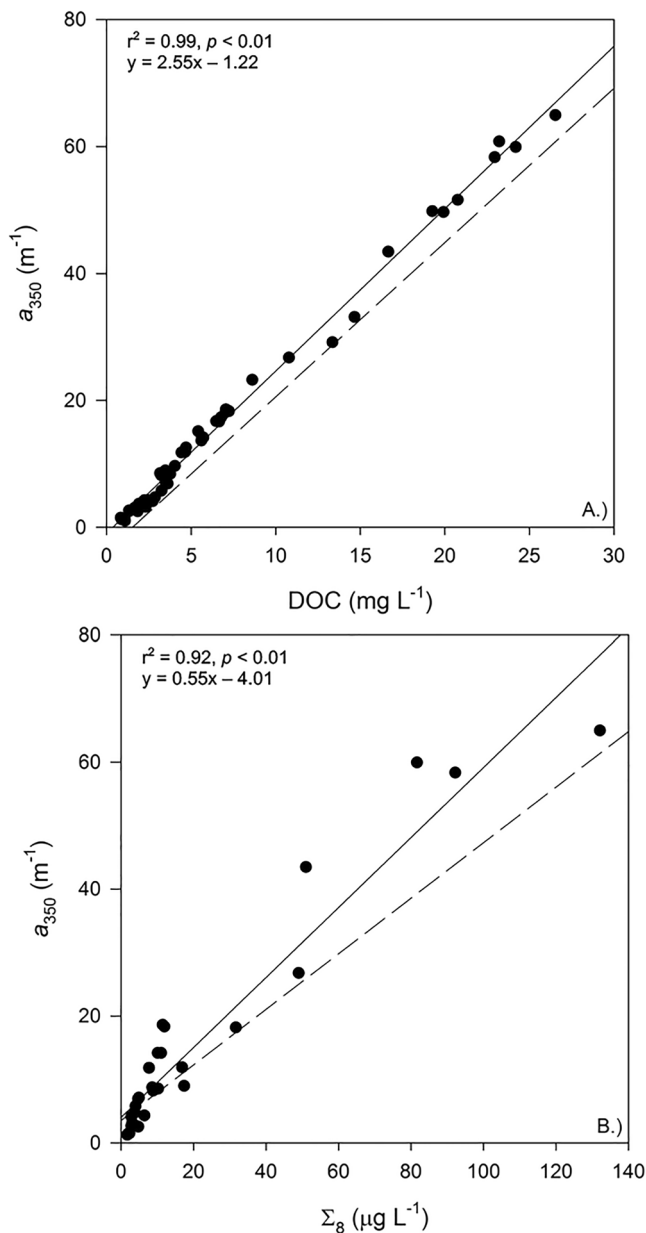
Figure 7. Relationship between a_{350} and (a) DOC concentration (black dots, solid line) and (b) lignin concentration (black dots, solid line) compared to the previously established Yukon River Basin relationships (dashed line) from Spencer et al. (2008).

may explain high DOC bioavailability previously observed during freshet (Behnke et al., 2021; Holmes et al., 2008; Textor et al., 2019; Wickland et al., 2012).

In addition to correlations with bulk DOM characteristics, optical parameters have been shown to strongly correlate with lignin phenol biomarkers (Benner & Kaiser, 2010; Hernes et al., 2009; Osburn & Stedmon, 2011; Spencer et al., 2009). A significant positive relationship between a_{350} and Σ_8 was observed across sites ($r^2 = 0.92$, $p < 0.01$; Figure 7b), similar to a previously described relationship from the Yukon River (Spencer et al., 2008). While the link between a_{350} and Σ_8 has been well established, relating lignin biomarkers to DOM molecular composition has been less well studied. Aromatic molecular formulae with high O/C ratios in the polyphenolic and condensed aromatic compound classes were positively correlated with Σ_8 (Figure 6f), indicating that the ranges typically used to classify molecular formulae as terrestrially derived are indeed broadly representative of terrestrial vegetation. Spearman rank correlations between molecular formulae and Σ_8 show terrestrially derived DOM is associated with aromatic molecular formulae, and that as lignin concentrations and yields increase with Q (i.e., during freshet), aromatic DOM with high O/C ratios is mobilized (Figures 3a–3f and 6f). These results show that optical parameters are strong predictors of DOM aromaticity, and that molecular composition measured via FT-ICR MS is significantly correlated with quantitative lignin biomarker analyses.

4.4. Landscape Controls on DOC Fluxes and Yields

The DOC yields from these sites were strongly correlated with watershed characteristics, such as basin slope ($r^2 = 0.69$, $p < 0.05$), consistent with previous studies (Connolly et al., 2018; Mutschlecner et al., 2018). The sites underlain by continuous permafrost had shallower maximum ALT and lower DOC yields compared to sites with higher DOC yields that were underlain by discontinuous permafrost ($r^2 = 0.37$, $p < 0.05$). These observations are consistent with yields observed by Frederick et al. (2012) where Arctic basins with shallower ALT had lower DOC yields. Watershed DOC yield was negatively correlated with the mean annual water yield ($r^2 = 0.80$, $p < 0.05$; Table 1) indicating that watersheds with lower water yields exported more DOC per km^2. Sites that had lower contribution of terrestrial DOM based on the relative abundance of condensed aromatic and polyphenolic molecular formulae and Σ_8 also exhibited lower DOC yield. If groundwater discharge increases with permafrost thaw, the DOC yield from these sites may remain low, with the caveat that deeper ALT can also increase the contribution of supra-permafrost groundwater, thus changing DOC yields dependent on the variable OC content of deeper soil horizons (Connolly et al., 2020; O'Donnell et al., 2012; Striegl et al., 2005).

4.5. Implications for Northern High-Latitude Streams and Rivers

Across the six rivers in Alaska we observed the impact of seasonality, permafrost cover, and landscape characteristics on DOM composition and DOC yields. The shallower active layer observed in the more northern sites (Atigun and Sagavanirktok) were accompanied by lower DOC concentrations and yields (Table 1), with DOM associated with autochthonous or non-vascular plant production rather than allochthonous, vascular plant sources (Figures 5 and 6d). Across the landscape, the sites with shallower watershed relief and deeper active layer were correlated with indicators of more aromatic DOM (Figures 6b and 6c). We

suggest that as temperatures warm, vegetation changes, and the active layer deepens, there will be associated shifts in DOM exported by rivers. Particularly in regions with high soil organic carbon content, DOM may shift toward greater export of terrestrial DOM consistent with higher fluxes of water soluble organic carbon from soils (Kane et al., 2006). However, the increase in groundwater contribution when water yield is low may also contribute more to shifts in DOM composition that are associated with less aromatic DOM (Figures 6a and 6b) exerting a seasonal and hydrologic control on DOM composition. As temperatures warm across the Arctic and boreal regions, vegetation shifts are projected, including the northward progression of the treeline, concurrent with the deepening of the active layer (Jorgenson et al., 2013; Neff & Hooper, 2002; Pearson et al., 2013) and warmer soils which can influence soil organic matter composition (Chen et al., 2018). Our data indicate that such shifts will lead to increased DOC flux and changes in DOM composition, particularly during the freshet when we observe higher $SUVA_{254}$, lignin phenol concentrations and yields, and increased relative abundances of polyphenolic molecular formulae. Meanwhile, during low flow conditions through the remainder of the ice-free season when sub-permafrost groundwater has a greater contribution to streamflow, DOM may shift toward less aromatic DOM composition as permafrost thaw deepens the active layer and warmer soil temperatures increase the interaction of groundwater flow with mineral soil layers. These results highlight the complexities of delineating the numerous impacts of climate change as this region experiences concurrent shifting vegetation, permafrost thaw, and changing riverine discharge.

Data Availability Statement

All data presented in this manuscript are available in the tables and Supporting Information S1 and are available through Open Science Framework (DOI: 10.17605/OSF.IO/DWG9K).

References

Abbott, B. W., Jones, J. B., Schuur, E. A. G., Chapin, III, F. S., Bowden, W. B., Bret-Harte, M. S., et al. (2016). Biomass offsets little or none of permafrost carbon release from soils, streams, and wildfire: An expert assessment. *Environmental Research Letters*, *11*, 034014. https://doi.org/10.1088/1748-9326/11/3/034014

ACIA. (2004). *Impacts of a warming Arctic: Arctic climate impact assessment*. Cambridge University Press.

Amon, R. M. W., Rinehart, A. J., Duan, S., Louchouarn, P., Prokushkin, A., Guggenberger, G., et al. (2012). Dissolved organic matter sources in large Arctic rivers. *Geochimica et Cosmochimica Acta*, *94*, 217–237. https://doi.org/10.1016/j.gca.2012.07.015

Battin, T. J., Luyssaert, S., Kaplan, L. A., Aufdenkampe, A. K., Richter, A., & Tranvik, L. J. (2009). The boundless carbon cycle. *Nature Geoscience*, *2*, 598–600. https://doi.org/10.1038/ngeo618

Behnke, M. I., McClelland, J. W., Tank, S. E., Kellerman, A. M., Holmes, R. M., Haghipour, N., et al. (2021). Pan-Arctic riverine dissolved organic matter: Synchronous molecular stability, shifting sources and subsidies. *Global Biogeochemical Cycles*, *35*(4), e2020GB006871. https://doi.org/10.1029/2020GB006871

Benner, R., & Kaiser, K. (2010). Biological and photochemical transformations of amino acids and lignin phenols in riverine dissolved organic matter. *Biogeochemistry*, *102*, 209–222. https://doi.org/10.1007/s10533-010-9435-4

Blakney, G. T., Hendrickson, C. L., & Marshall, A. G. (2011). Predator data station: A fast data acquisition system for advanced FT-ICR MS experiments. *International Journal of Mass Spectrometry*, *306*(2–3), 246–252. https://doi.org/10.1016/j.ijms.2011.03.009

Bring, A., Fedorova, I., Dibike, Y., others, L., Mård, J., Mernild, S. H., et al. (2016). Arctic terrestrial hydrology: A synthesis of processes, regional effects, and research challenges. *Journal of Geophysical Research: Biogeosciences*, *121*, 621–649. https://doi.org/10.1002/2015JG003131

Carey, J. C., Gewirtzman, J., Johnston, S. E., Kurtz, A., Tang, J., Vieillard, A. M., & Spencer, R. G. M. (2020). Arctic River dissolved and biogenic silicon exports—Current conditions and future changes with warming. *Global Biogeochemical Cycles*, *34*(3), e2019GB006308. https://doi.org/10.1029/2019GB006308

Casas-Ruiz, J. P., Spencer, R. G. M., Guillemette, F., von Schiller, D., Obrador, B., Podgorski, D. C., et al. (2020). Delineating the continuum of dissolved organic matter in temperate river networks. *Global Biogeochemical Cycles*, *34*(8), e2019GB006495. https://doi.org/10.1029/2019GB006495

Chen, H., Yang, Z., Chu, R. K., Tolic, N., Liang, L., Graham, D. E., et al. (2018). Molecular insights into Arctic soil organic matter degradation under warming. *Environmental Science & Technology*, *52*(8), 4555–4564. https://doi.org/10.1021/acs.est.7b05469

Cole, J. J., Prairie, Y. T., Caraco, N. F., McDowell, W. H., Tranvik, L. J., Striegl, R. G., et al. (2007). Plumbing the global carbon cycle: Integrating inland waters into the terrestrial carbon budget. *Ecosystems*, *10*, 172–185. https://doi.org/10.1007/s10021-006-9013-8

Connolly, C. T., Cardenas, M. B., Burkart, G. A., Spencer, R. G. M., & McClelland, J. W. (2020). Groundwater as a major source of dissolved organic matter to Arctic coastal waters. *Nature Communications*, *11*(1), 1479. https://doi.org/10.1038/s41467-020-15250-8

Connolly, C. T., Khosh, M. S., Burkart, G. A., Douglas, T. A., Holmes, R. M., Jacobson, A. D., et al. (2018). Watershed slope as a predictor of fluvial dissolved organic matter and nitrate concentrations across geographical space and catchment size in the Arctic. *Environmental Research Letters*, *13*, 104015. https://doi.org/10.1088/1748-9326/aae35d

Corilo, Y. (2015). *EnviroOrg Software E 2.1*. Florida State University.

Cory, R. M., & McKnight, D. M. (2005). Fluorescence spectroscopy reveals ubiquitous presence of oxidized and reduced quinones in dissolved organic matter. *Environmental science & technology*, *39*, 8142–8149. https://doi.org/10.1021/es0506962

D'Andrilli, J., Cooper, W. T., Foreman, C. M., & Marshall, A. G. (2015). An ultrahigh-resolution mass spectrometry index to estimate natural organic matter lability. *Rapid Communications in Mass Spectrometry*, *29*, 2385–2401. https://doi.org/10.1002/rcm.7400

Dittmar, T., Koch, B., Hertkorn, N., & Kattner, G. (2008). A simple and efficient method for the solid-phase extraction of dissolved organic matter (SPE-DOM) from seawater. *Limnology and Oceanography: Methods*, *6*, 230–235. https://doi.org/10.4319/lom.2008.6.230

Drake, T. W., Raymond, P. A., & Spencer, R. G. M. (2018). Terrestrial carbon inputs to inland waters: A current synthesis of estimates and uncertainty. *Limnology and Oceanography Letters*, *3*(3), 132–142. https://doi.org/10.1002/lol2.10055

Drake, T. W., Wickland, K. P., Spencer, R. G. M., McKnight, D. M., & Striegl, R. G. (2015). Ancient low–molecular-weight organic acids in permafrost fuel rapid carbon dioxide production upon thaw. *Proceedings of the National Academy of Sciences*, *112*, 13946–13951. https://doi.org/10.1073/pnas.1511705112

Feng, X., Vonk, J. E., Griffin, C., Zimov, N., Montluçon, D. B., Wacker, L., & Eglinton, T. I. (2017). ^{14}C Variation of dissolved lignin in arctic river systems. *ACS Earth and Space Chemistry*, *1*(6), 334–344. https://doi.org/10.1021/acsearthspacechem.7b00055

Frederick, Z. A., Anderson, S. P., & Striegl, R. G. (2012). Annual estimates of water and solute export from 42 tributaries to the Yukon River. *Hydrological Processes*, *26*, 1949–1961. https://doi.org/10.1002/hyp.8255

Frey, K. E., & McClelland, J. W. (2009). Impacts of permafrost degradation on arctic river biogeochemistry. *Hydrological Processes*, *23*, 169–182. https://doi.org/10.1002/hyp.7196

Griffin, C. G., McClelland, J. W., Frey, K. E., Fiske, G., & Holmes, R. M. (2018). Quantifying CDOM and DOC in major Arctic rivers during ice-free conditions using Landsat TM and ETM+ data. *Remote Sensing of Environment*, *209*, 395–409. https://doi.org/10.1016/j.rse.2018.02.060

Harms, T. K., Edmonds, J. W., Genet, H., Creed, I. F., Aldred, D., Balser, A., & Jones, J. B. (2016). Catchment influence on nitrate and dissolved organic matter in Alaskan streams across a latitudinal gradient. *Journal of Geophysical Research: Biogeosciences*, *121*, 350–369. https://doi.org/10.1002/2015JG003201

Hedges, J. I., & Mann, D. C. (1979). The characterization of plant tissues by their lignin oxidation products. *Geochimica et Cosmochimica Acta*, *43*, 1803–1807. https://doi.org/10.1016/0016-7037(79)90028-0

Helms, J. R., Stubbins, A., Ritchie, J. D., Minor, E. C., Kieber, D. J., & Mopper, K. (2008). Absorption spectral slopes and slope ratios as indicators of molecular weight, source, and photobleaching of chromophoric dissolved organic matter. *Limnology & Oceanography*, *53*, 955–969. https://doi.org/10.4319/lo.2008.53.3.0955

Hendrickson, C. L., Quinn, J. P., Kaiser, N. K., Smith, D. F., Blakney, G. T., Chen, T., et al. (2015). 21 Tesla Fourier transform ion cyclotron resonance mass spectrometer: A national resource for ultrahigh resolution mass analysis. *Journal of the American Society for Mass Spectrometry*, *26*, 1626–1632. https://doi.org/10.1007/s13361-015-1182-2

Hernes, P. J., & Benner, R. (2002). Transport and diagenesis of dissolved and particulate terrigenous organic matter in the North Pacific Ocean. *Deep Sea Research Part I: Oceanographic Research Papers*, *49*(12), 2119–2132. https://doi.org/10.1016/S0967-0637(02)00128-0

Hernes, P. J., & Benner, R. (2003). Photochemical and microbial degradation of dissolved lignin phenols: Implications for the fate of terrigenous dissolved organic matter in marine environments. *Journal of Geophysical Research*, *108*. https://doi.org/10.1029/2002JC001421

Hernes, P. J., Bergamaschi, B. A., Eckard, R. S., & Spencer, R. G. M. (2009). Fluorescence-based proxies for lignin in freshwater dissolved organic matter. *Journal of Geophysical Research*, *114*. https://doi.org/10.1029/2009JG000938

Hernes, P. J., Robinson, A. C., & Aufdenkampe, A. K. (2007). Fractionation of lignin during leaching and sorption and implications for organic matter "freshness." *Geophysical Research Letters*, *34*(17). https://doi.org/10.1029/2007GL031017

Holmes, R. M., McClelland, J. W., Peterson, B. J., Tank, S. E., Bulygina, E., Eglinton, T. I., et al. (2012). Seasonal and annual fluxes of nutrients and organic matter from large rivers to the Arctic Ocean and surrounding seas. *Estuaries and Coasts*, *35*, 369–382. https://doi.org/10.1007/s12237-011-9386-6

Holmes, R. M., McClelland, J. W., Raymond, P. A., Frazer, B. B., Peterson, B. J., & Stieglitz, M. (2008). Lability of DOC transported by Alaskan rivers to the Arctic Ocean. *Geophysical Research Letters*, *35*(3). https://doi.org/10.1029/2007GL032837

Hu, F. S., Higuera, P. E., Walsh, J. E., Chapman, W. L., Duffy, P. A., Brubaker, L. B., & Chipman, M. L. (2010). Tundra burning in Alaska: Linkages to climatic change and sea ice retreat. *Journal of Geophysical Research*, *115*, G04002. https://doi.org/10.1029/2009JG001270

Johnston, S. E., Bogard, M. J., Rogers, J. A., Butman, D., Striegl, R. G., Dornblaser, M., & Spencer, R. G. M. (2019). Constraining dissolved organic matter sources and temporal variability in a model sub-Arctic lake. *Biogeochemistry*, *146*(3), 271–292. https://doi.org/10.1007/s10533-019-00619-9

Johnston, S. E., Shorina, N., Bulygina, E., Vorobjeva, T., Chupakova, A., Klimov, S. I., et al. (2018). Flux and seasonality of dissolved organic matter from the Northern Dvina (Severnaya Dvina) River, Russia. *Journal of Geophysical Research: Biogeosciences*, *123*, 1041–1056. https://doi.org/10.1002/2017JG004337

Jorgenson, M. T., Harden, J., Kanevskiy, M., O'Donnell, J., Wickland, K., Ewing, S., et al. (2013). Reorganization of vegetation, hydrology and soil carbon after permafrost degradation across heterogeneous boreal landscapes. *Environmental Research Letters*, *8*, 035017. https://doi.org/10.1088/1748-9326/8/3/035017

Jorgenson, M. T., Racine, C. H., Walters, J. C., & Osterkamp, T. E. (2001). *Permafrost Degradation and Ecological Changes Associated with a Warming Climate in Central Alaska*. (Vol. 29).

Kaiser, K., Canedo-Oropeza, M., McMahon, R., & Amon, R. M. W. (2017). Origins and transformations of dissolved organic matter in large Arctic rivers. *Scientific Reports*, *7*(1), 13064. https://doi.org/10.1038/s41598-017-12729-1

Kaiser, K., & Guggenberger, G. (2000). The role of DOM sorption to mineral surfaces in the preservation of organic matter in soils. *Organic Geochemistry*, *31*, 711–725. https://doi.org/10.1016/S0146-6380(00)00046-2

Kane, E. S., Valentine, D. W., Michaelson, G. J., Fox, J. D., & Ping, C.-L. (2006). Controls over pathways of carbon efflux from soils along climate and black spruce productivity gradients in interior Alaska. *Soil Biology and Biochemistry*, *38*(6), 1438–1450. https://doi.org/10.1016/j.soilbio.2005.11.004

Kane, E. S., Valentine, D. W., Schuur, E. A., & Dutta, K. (2005). Soil carbon stabilization along climate and stand productivity gradients in black spruce forests of interior Alaska. *Canadian Journal of Forest Research*, *35*(9), 2118–2129. https://doi.org/10.1139/x05-093

Kawahigashi, M., Kaiser, K., Kalbitz, K., Rodionov, A., & Guggenberger, G. (2004). Dissolved organic matter in small streams along a gradient from discontinuous to continuous permafrost: DOM in tributaries along a permafrost gradient. *Global Change Biology*, *10*(9), 1576–1586. https://doi.org/10.1111/j.1365-2486.2004.00827.x

Kellerman, A. M., Dittmar, T., Kothawala, D. N., & Tranvik, L. J. (2014). Chemodiversity of dissolved organic matter in lakes driven by climate and hydrology. *Nature Communications*, *5*, 3804. https://doi.org/10.1038/ncomms4804

Kellerman, A. M., Guillemette, F., Podgorski, D. C., Aiken, G. R., Butler, K. D., & Spencer, R. G. M. (2018). Unifying concepts linking dissolved organic matter composition to persistence in aquatic ecosystems. *Environmental Science & Technology*, *52*, 2538–2548. https://doi.org/10.1021/acs.est.7b05513

Koch, B. P., & Dittmar, T. (2006). From mass to structure: An aromaticity index for high-resolution mass data of natural organic matter. *Rapid Communications in Mass Spectrometry*, *20*, 926–932. https://doi.org/10.1002/rcm.2386

Koch, B. P., & Dittmar, T. (2016). From mass to structure: An aromaticity index for high-resolution mass data of natural organic matter. *Rapid Communications in Mass Spectrometry*, *30*, 250–250. https://doi.org/10.1002/rcm.7433

Koch, J. C., Kikuchi, C. P., Wickland, K. P., & Schuster, P. (2014). Runoff sources and flow paths in a partially burned, upland boreal catchment underlain by permafrost. *Water Resources Research*, *50*, 8141–8158. https://doi.org/10.1002/2014WR015586

Koch, J. C., Runkel, R. L., Striegl, R., & McKnight, D. M. (2013). Hydrologic controls on the transport and cycling of carbon and nitrogen in a boreal catchment underlain by continuous permafrost. *Journal of Geophysical Research: Biogeosciences*, *118*, 698–712. https://doi.org/10.1002/jgrg.20058

Kujawinski, E. B. (2002). Electrospray Ionization Fourier Transform Ion Cyclotron Resonance Mass Spectrometry (ESI FT-ICR MS): Characterization of complex environmental mixtures. *Environmental Forensics*, *3*(3), 207–216. https://doi.org/10.1006/enfo.2002.0109

Lester, R. E., Close, P. G., Barton, J. L., Pope, A. J., & Brown, S. C. (2014). Predicting the likely response of data-poor ecosystems to climate change using space-for-time substitution across domains. *Global Change Biology*, *20*(11), 3471–3481. https://doi.org/10.1111/gcb.12634

Loranty, M. M., Abbott, B. W., Blok, D., Douglas, T. A., Epstein, H. E., Forbes, B. C., et al. (2018). Reviews and syntheses: Changing ecosystem influences on soil thermal regimes in northern high-latitude permafrost regions. *Biogeosciences*, *15*(17), 5287–5313. https://doi.org/10.5194/bg-15-5287-2018

Mann, P. J., Davydova, A., Zimov, N., Spencer, R. G. M., Davydov, S., Bulygina, E., et al. (2012). Controls on the composition and lability of dissolved organic matter in Siberia's Kolyma River basin. *Journal of Geophysical Research*, *117*. https://doi.org/10.1029/2011JG001798

Mann, P. J., Spencer, R. G. M., Hernes, P. J., Six, J., Aiken, G. R., Tank, S. E., et al. (2016). Pan-Arctic trends in terrestrial dissolved organic matter from optical measurements. *Frontiers in Earth Science*, *25*. https://doi.org/10.3389/feart.2016.00025

Massicotte, P., Asmala, E., Stedmon, C., & Markager, S. (2017). Global distribution of dissolved organic matter along the aquatic continuum: Across rivers, lakes and oceans. *The Science of the Total Environment*, *609*, 180–191. https://doi.org/10.1016/j.scitotenv.2017.07.076

McClelland, J. W., Stieglitz, M., Pan, F., Holmes, R. M., & Peterson, B. J. (2007). Recent changes in nitrate and dissolved organic carbon export from the upper Kuparuk River, North Slope, Alaska: N and C export from the Kuparuk River. *Journal of Geophysical Research*, *112*. https://doi.org/10.1029/2006JG000371

McGuire, A. D., Anderson, L. G., Christensen, T. R., Dallimore, S., Guo, L., Hayes, D. J., et al. (2009). Sensitivity of the carbon cycle in the Arctic to climate change. *Ecological Monographs 79*: 523–555. https://doi.org/10.1890/08-2025.1

McKnight, D. M., Boyer, E. W., Westerhoff, P. K., Doran, P. T., Kulbe, T., & Andersen, D. T. (2001). Spectrofluorometric characterization of dissolved organic matter for indication of precursor organic material and aromaticity. *Limnology & Oceanography*, *46*, 38–48. https://doi.org/10.4319/lo.2001.46.1.0038

Moingt, M., Lucotte, M., & Paquet, S. (2016). Lignin biomarkers signatures of common plants and soils of Eastern Canada. *Biogeochemistry*, *129*(1), 133–148. https://doi.org/10.1007/s10533-016-0223-7

Murphy, K., Stedmon, C. A., Graeber, D., & Bro, R. (2013). Fluorescence spectroscopy and multi-way techniques. *PARAFAC Analytical Methods*, *5*, 6557–6566. https://doi.org/10.1039/C3AY41160E

Mutschlecner, A. E., Guerard, J. J., Jones, J. B., & Harms, T. K. (2018). Regional and intra-annual stability of dissolved organic matter composition and biolability in high-latitude Alaskan rivers. *Limnology and Oceanography*, *63*(4), 1605–1621. https://doi.org/10.1002/lno.10795

Neff, J. C., & Hooper, D. U. (2002). Vegetation and climate controls on potential CO_2, DOC and DON production in northern latitude soils. *Global Change Biology*, *8*, 872–884. https://doi.org/10.1046/j.1365-2486.2002.00517.x

O'Donnell, J. A., Aiken, G. R., Butler, K. D., Guillemette, F., Podgorski, D. C., & Spencer, R. G. M. (2016). DOM composition and transformation in boreal forest soils: The effects of temperature and organic-horizon decomposition state. *Journal of Geophysical Research: Biogeosciences*, *121*, 2727–2744. https://doi.org/10.1002/2016JG003431

O'Donnell, J. A., Aiken, G. R., Kane, E. S., & Jones, J. B. (2010). Source water controls on the character and origin of dissolved organic matter in streams of the Yukon River basin, Alaska. *Journal of Geophysical Research*, *115*, G03025. https://doi.org/10.1029/2009JG001153

O'Donnell, J. A., Aiken, G. R., Walvoord, M. A., & Butler, K. D. (2012). Dissolved organic matter composition of winter flow in the Yukon River basin: Implications of permafrost thaw and increased groundwater discharge. *Global Biogeochemical Cycles*, *26*, GB0E06. https://doi.org/10.1029/2012GB004341

O'Donnell, J. A., Aiken, G. R., Walvoord, M. A., Raymond, P. A., Butler, K. D., Dornblaser, M. M., & Heckman, K. (2014). Using dissolved organic matter age and composition to detect permafrost thaw in boreal watersheds of interior Alaska. *Journal of Geophysical Research: Biogeosciences*, *119*, 2155–2170. https://doi.org/10.1002/2014JG002695

Osburn, C. L., & Stedmon, C. A. (2011). Linking the chemical and optical properties of dissolved organic matter in the Baltic–North Sea transition zone to differentiate three allochthonous inputs. *Marine Chemistry*, *126*, 281–294. https://doi.org/10.1016/j.marchem.2011.06.007

Pearson, R. G., Phillips, S. J., Loranty, M. M., Beck, P. S. A., Damoulas, T., Knight, S. J., & Goetz, S. J. (2013). Shifts in Arctic vegetation and associated feedbacks under climate change. *Nature Climate Change*, *3*, 673–677. https://doi.org/10.1038/nclimate1858

Pellerin, B. A., Saraceno, J. F., Shanley, J. B., Sebestyen, S. D., Aiken, G. R., Wollheim, W. M., & Bergamaschi, B. A. (2012). Taking the pulse of snowmelt: In situ sensors reveal seasonal, event and diurnal patterns of nitrate and dissolved organic matter variability in an upland forest stream. *Biogeochemistry*, *108*, 183–198. https://doi.org/10.1007/s10533-011-9589-8

Raymond, P. A., McClelland, J. W., Holmes, R. M., Zhulidov, A. V., Mull, K., Peterson, B. J., et al. (2007). Flux and age of dissolved organic carbon exported to the Arctic Ocean: A carbon isotopic study of the five largest arctic rivers. *Global Biogeochemical Cycles*, *21*, GB4011. https://doi.org/10.1029/2007GB002934

Rodríguez-Cardona, B. M., Coble, A. A., Wymore, A. S., Kolosov, R., Podgorski, D. C., Zito, P., et al. (2020). Wildfires lead to decreased carbon and increased nitrogen concentrations in upland arctic streams. *Scientific Reports*, *10*(1), 8722. https://doi.org/10.1038/s41598-020-65520-0

Runkel, R. L., Crawford, C. G., & Cohn, T. A. (2004). Load Estimator (LOADEST): A FORTRAN program for estimating constituent loads in streams and rivers. In *Techniques and methods Book 4*. U.S. Geological Survey. https://doi.org/10.3133/tm4a5

Schuur, E. A. G., Abbott, B. W., Bowden, W. B., Brovkin, V., Camill, P., Canadell, J. G., et al. (2013). Expert assessment of vulnerability of permafrost carbon to climate change. *Climatic Change*, *119*, 359–374. https://doi.org/10.1007/s10584-013-0730-7

Smith, D. F., Podgorski, D. C., Rodgers, R. P., Blakney, G. T., & Hendrickson, C. L. (2018). 21 Tesla FT-ICR Mass Spectrometer for ultrahigh-resolution analysis of complex organic mixtures. *Analytical Chemistry*, *90*, 2041–2047. https://doi.org/10.1021/acs.analchem.7b04159

Spencer, R. G. M., Aiken, G. R., Butler, K. D., Dornblaser, M. M., Striegl, R. G., & Hernes, P. J. (2009). Utilizing chromophoric dissolved organic matter measurements to derive export and reactivity of dissolved organic carbon exported to the Arctic Ocean: A case study of the Yukon River, Alaska. *Geophysical Research Letters*, *36*. https://doi.org/10.1029/2008gl036831

Spencer, R. G. M., Aiken, G. R., Dyda, R. Y., Butler, K. D., Bergamaschi, B. A., & Hernes, P. J. (2010). Comparison of XAD with other dissolved lignin isolation techniques and a compilation of analytical improvements for the analysis of lignin in aquatic settings. *Organic Geochemistry*, *41*, 445–453. https://doi.org/10.1016/j.orggeochem.2010.02.004

Spencer, R. G. M., Aiken, G. R., Wickland, K. P., Striegl, R. G., & Hernes, P. J. (2008). Seasonal and spatial variability in dissolved organic matter quantity and composition from the Yukon River basin, Alaska: Yukon River Basin DOM Dynamics. *Global Biogeochemical Cycles*, *22*. https://doi.org/10.1029/2008GB003231

Spencer, R. G. M., Mann, P. J., Dittmar, T., Eglinton, T. I., McIntyre, C., Holmes, R. M., et al. (2015). Detecting the signature of permafrost thaw in Arctic rivers. *Geophysical Research Letters*, *42*. https://doi.org/10.1002/2015GL063498

Spencer, R. G. M., Pellerin, B. A., Bergamaschi, B. A., Downing, B. D., Kraus, T. E. C., Smart, D. R., et al. (2007). Diurnal variability in riverine dissolved organic matter composition determined by in situ optical measurement in the San Joaquin River (California, USA). *Hydrological Processes*, *21*, 3181–3189. https://doi.org/10.1002/hyp.6887

Stedmon, C. A., Amon, R. M. W., Rinehart, A. J., & Walker, S. A. (2011). The supply and characteristics of colored dissolved organic matter (CDOM) in the Arctic Ocean: Pan Arctic trends and differences. *Marine Chemistry*, *124*, 108–118. https://doi.org/10.1016/j.marchem.2010.12.007

Striegl, R. G., Aiken, G. R., Dornblaser, M. M., Raymond, P. A., & Wickland, K. P. (2005). A decrease in discharge-normalized DOC export by the Yukon River during summer through autumn. *Geophysical Research Letters*, *32*, L21413. https://doi.org/10.1029/2005GL024413

Striegl, R. G., Dornblaser, M. M., Aiken, G. R., Wickland, K. P., & Raymond, P. A. (2007). Carbon export and cycling by the Yukon, Tanana, and Porcupine rivers, Alaska, 2001–2005. *Water Resources Research*, *43*, W02411. https://doi.org/10.1029/2006WR005201

Stubbins, A., Spencer, R. G. M., Mann, P. J., Holmes, R. M., McClelland, J. W., Niggemann, J., & Dittmar, T. (2015). Utilizing colored dissolved organic matter to derive dissolved black carbon export by arctic rivers. *Marine Biogeochemistry*, *63*. https://doi.org/10.3389/feart.2015.00063

Textor, S. R., Wickland, K. P., Podgorski, D. C., Johnston, S. E., & Spencer, R. G. M. (2019). Dissolved Organic carbon turnover in permafrost-influenced watersheds of interior Alaska: Molecular insights and the priming effect. *Frontiers of Earth Science*, *7*, 275. https://doi.org/10.3389/feart.2019.00275

Verpoorter, C., Kutser, T., Seekell, D. A., & Tranvik, L. J. (2014). A global inventory of lakes based on high-resolution satellite imagery. *Geophysical Research Letters*, *41*, 6396–6402. https://doi.org/10.1002/2014GL060641

Vonk, J. E., Tank, S. E., Bowden, W. B., Laurion, I., Vincent, W. F., Alekseychik, P., et al. (2015). Reviews and syntheses: Effects of permafrost thaw on Arctic aquatic ecosystems. *Biogeosciences*, *12*, 7129–7167. https://doi.org/10.5194/bg-12-7129-2015

Vonk, J. E., Tank, S. E., Mann, P. J., Spencer, R. G. M., Treat, C. C., Striegl, R. G., et al. (2015). Biodegradability of dissolved organic carbon in permafrost soils and aquatic systems: A meta-analysis. *Biogeosciences*, *12*, 6915–6930. https://doi.org/10.5194/bg-12-6915-2015

Waggoner, D. C., Chen, H., Willoughby, A. S., & Hatcher, P. G. (2015). Formation of black carbon-like and alicyclic aliphatic compounds by hydroxyl radical initiated degradation of lignin. *Organic Geochemistry*, *82*, 69–76. https://doi.org/10.1016/j.orggeochem.2015.02.007

Walvoord, M. A., & Striegl, R. G. (2007). Increased groundwater to stream discharge from permafrost thawing in the Yukon River basin: Potential impacts on lateral export of carbon and nitrogen. *Geophysical Research Letters*, *34*, L12402. https://doi.org/10.1029/2007GL030216

Walvoord, M. A., Voss, C. I., & Wellman, T. P. (2012). Influence of permafrost distribution on groundwater flow in the context of climate-driven permafrost thaw: Example from Yukon Flats Basin, Alaska, United States. *Water Resource Research*, *48*. https://doi.org/10.1029/2011WR011595

Weishaar, J. L., Aiken, G. R., Bergamaschi, B. A., Fram, M. S., Fujii, R., & Mopper, K. (2003). Evaluation of specific ultraviolet absorbance as an indicator of the chemical composition and reactivity of dissolved organic carbon. *Environmental Science & Technology*, *37*, 4702–4708. https://doi.org/10.1021/es030360x

Wickland, K. P., Aiken, G. R., Butler, K., Dornblaser, M. M., Spencer, R. G. M., & Striegl, R. G. (2012). Biodegradability of dissolved organic carbon in the Yukon River and its tributaries: Seasonality and importance of inorganic nitrogen. *Global Biogeochemical Cycles*, *26*, GB0E03. https://doi.org/10.1029/2012GB004342

Williams, C. J., Yavitt, J. B., Wieder, R. K., & Cleavitt, N. L. (1998). Cupric oxide oxidation products of northern peat and peat-forming plants. *Canadian Journal of Botany*, *76*(1), 51–62. https://doi.org/10.1139/b97-150